

1
2
3
4
5
6 **Comprehensive detection of structural variation and transposable element differences**
7 **between wild type laboratory lineages of *C. elegans***
8

9 Zachary D. Bush¹, Alice F. S. Naftaly¹, Devin Dinwiddie¹, Cora Albers¹, Kenneth J. Hillers², and
10 Diana E. Libuda^{1*}

11
12 ¹ Institute of Molecular Biology, Department of Biology, University of Oregon, 1229 Franklin Blvd
13 Eugene, OR 97403, USA

14 ² Biological Sciences Department, California Polytechnic State University, San Luis Obispo,
15 California, USA

16
17 *Corresponding author

18
19 Corresponding Author and Lead Contact Information:

20 Diana E. Libuda, PhD
21 University of Oregon
22 Institute of Molecular Biology
23 1229 Franklin Blvd
24 Eugene, OR 97403
25 541-346-5092 (phone)
26 541-346-4854 (fax)
27 dlibuda@uoregon.edu

28
29 Running title: Structural variations in *C. elegans* genomes
30 Keywords: genome stability; sequence variation; reference genomes; genetic drift;
31 transposons; whole genome sequencing; *C. elegans*

32 **Abstract**

33 Genomic structural variations (SVs) and transposable elements (TEs) can be significant
34 contributors to genome evolution, altered gene expression, and risk of genetic diseases. Recent
35 advancements in long-read sequencing have greatly improved the quality of *de novo* genome
36 assemblies and enhanced the detection of sequence variants at the scale of hundreds or
37 thousands of bases. Comparisons between two diverged wild isolates of *Caenorhabditis*
38 *elegans*, the Bristol and Hawaiian strains, have been widely utilized in the analysis of small
39 genetic variations. Genetic drift, including SVs and rearrangements of repeated sequences such
40 as TEs, can occur over time from long-term maintenance of wild type isolates within the
41 laboratory. To comprehensively detect both large and small structural variations as well as TEs
42 due to genetic drift, we generated *de novo* genome assemblies and annotations for each strain
43 from our lab collection using both long- and short-read sequencing and compared our
44 assemblies and annotations with that of other lab wild type strains. Within our lab assemblies,
45 we annotate over 3.1Mb of sequence divergence between the Bristol and Hawaiian isolates:
46 337,584 SNPs, 94,503 small insertion-deletions (<50bp), and 4,334 structural variations
47 (>50bp). Further, we define the location and movement of specific DNA TEs between N2 Bristol
48 and CB4856 Hawaiian wild type isolates. Specifically, we find the N2 Bristol genome has 20.6%
49 more TEs from the *Tc1/mariner* family than the CB4856 Hawaiian genome. Moreover, we
50 identified Zator elements as the most abundant and mobile TE family in the genome. Using
51 specific TE sequences with unique SNPs, we also identify 38 TEs that moved
52 intrachromosomally and 9 TEs that moved interchromosomally between the N2 Bristol and
53 CB4856 Hawaiian genomes. By comparing the *de novo* genome assembly of our lab collection
54 Bristol isolate to the VC2010 Bristol assembly, we also reveal that lab lineages display over 2
55 Mb of total variation: 1,162 SNPs, 1,528 indels, and 897 SVs with 95% of the variation due to
56 SVs. Overall, our work demonstrates the unique contribution of SVs and TEs to variation and

57 genetic drift between wild type laboratory strains assumed to be isogenic despite growing

58 evidence of genetic drift and phenotypic variation.

59 **Author Summary**

60 For multiple model organisms, propagation of wild type strains in independent labs can lead to
61 multiple phenotypic differences over time. To assess recombination, map mutations, and
62 understand genomic changes during speciation, *Caenorhabditis elegans* researchers primarily
63 use the wild type isolates Bristol and Hawaiian. Here, we map structural variations,
64 transposable elements, and sequence divergence between the Bristol and Hawaiian natural
65 isolates and between genomes of different lab lineages of these same strains.

66

67 **Introduction**

68 Genomic variants, through mutation and recombination, in individuals and genetic drift in
69 populations underly the core process of evolution. Functional characterization of sequence
70 variants guides our understanding of phenotypic variances within species while also being
71 critical to identifying heritable disease-causing mutations (Haraksingh and Snyder 2013).
72 Genomic variation has been reported at multiple scales, from single nucleotide polymorphisms
73 (SNPs) to short insertions/deletions (indels) to much larger structural variants (SVs). SVs are
74 defined as insertions, deletions, or chromosomal rearrangements at least 50bp in length. SVs
75 can cause loss of function mutations through large gene deletions or alter gene expression by
76 disrupting spatial interactions between regulatory sequences (Stranger et al. 2007; Hurles,
77 Dermitzakis, and Tyler-Smith 2008). Accurate detection of both sequence variants and
78 chromosome rearrangements is critical for understanding how genomic variation may contribute
79 to phenotypic plasticity in individuals and populations of the same species.

80 Transposable elements (TEs) are a class of repetitive DNA sequences capable of
81 moving to new locations in the genome. TE mobility is a source of genomic structural variation
82 that can also alter gene expression (Girard and Freeling 1999; Slotkin and Martienssen 2007)
83 and drive, sometimes rapid, evolutionary changes within species (Van't Hof et al. 2016;
84 Feschotte and Pritham 2007). Notably, transposons account for a significant fraction of the total
85 DNA sequence in many eukaryotic species (Chalopin et al. 2015; Gilbert, Peccoud, and
86 Cordaux 2021), which provides many opportunities for TE-driven structural rearrangements.
87 The *Tc1/mariner* family of DNA transposons is one of the most abundant TEs across species
88 (Eide and Anderson 1985; Plasterk, Izsvák, and Ivics 1999), and early studies in *C. elegans*
89 found it to be one of the few mobile transposons observed under laboratory conditions (Fischer,
90 Wienholds, and Plasterk 2003). To repress or limit transposon mobilization, transposon
91 silencing is tightly regulated through multiple mechanisms including chromatin modification and
92 RNA interference (Sijen and Plasterk 2003; H.-C. Lee et al. 2012). Despite their ubiquity and

93 impact on genomic architecture, the comprehensive annotation and inclusion of TEs in
94 comparative genomic analyses has been challenging. Many studies have incompletely
95 characterized the genomic distribution of TEs because older, short-read based genome
96 assemblies could not accurately map the full content of repetitive sequences. Further, programs
97 that automatically detect TEs based on sequence homology and conserved sequence elements
98 rely heavily on libraries of older reference sequences that may predate the discovery of TE
99 fragments and newer TE families. As new families of transposable elements are discovered
100 (Bao et al. 2009) along with new technology that aids their annotation and tracking (Riehl et al.
101 2022), determining the genomic composition and mobility of new TEs will enable our
102 understanding of their role in genome evolution and genome integrity.

103 Foundational research on genomic variation has utilized next generation short-read
104 sequencing, long-read sequencing, and the direct comparison of reference genome assemblies
105 to identify genomic variants (Mahmoud et al. 2019; Lappalainen et al. 2019). SNPs and indels,
106 ranging in size from 1 bp to 50bp, can be identified with high confidence using short sequencing
107 reads that are 100-150bp (Muzzey, Evans, and Lieber 2015). In contrast, SVs are challenging to
108 annotate using short-read sequencing because the sequencing reads are often smaller than the
109 size of an SV (Sudmant et al. 2015; Mahmoud et al. 2019; Lesack et al. 2022). Similarly, the
110 highly repetitive sequences of TEs present significant challenges to mapping and annotation
111 with traditional short read sequencing methods. With the advent of higher quality long-read
112 sequencing technologies which generate ~10kb-30kb reads with lower genomic coverage, the
113 accurate annotation of large regions of genomic variation such as SVs and transposable
114 elements has become easier (Sakamoto et al. 2021). New tools to identify SVs via assembly-to-
115 assembly alignments (Delcher et al. 1999; Nattestad and Schatz 2016; Li 2018; Goel et al.
116 2019) are not constrained by read-length to identify SVs and depend on high-quality reference
117 assemblies. Thus, a high-quality reference genome assembly is a critical resource for any
118 model organism. Methods of variant detection that leverage a combined utilization of short- and

119 long-read sequencing can provide more accurate reference sequences to fully address
120 undiscovered genomic variations previously not detected by short-read sequencing alone.

121 *Caenorhabditis elegans* was the first multicellular organism to have its genome fully
122 sequenced (C. elegans Sequencing Consortium 1998) and has been exploited to pioneer many
123 comparative genomic studies. To understand how genetic variation influences phenotypic
124 differences and genomic processes within species, *C. elegans* researchers primarily utilize two
125 highly diverged wild type strains estimated to have diverged 30,000-50,000 generations ago
126 (Thomas et al. 2015): N2 (isolated in Bristol, England) and CB4856 (isolated in Maui, Hawaii)
127 (Nicholas, Dougherty, and Hansen 1959; Sulston and Brenner 1974; Hodgkin and Doniach
128 1997; Crombie et al. 2019). Earlier comparisons of the Bristol and Hawaiian lineages were
129 critical for studying genetic variation, gene families, and evolution of genome structures (Koch et
130 al. 2000; Wicks et al. 2001; Stewart et al. 2005; Maydan et al. 2010). The *C. elegans* genome,
131 comprised of 5 autosomes and the X chromosome, displays a nonuniform distribution of
132 sequence variation when comparing the genomes of wild isolates. Although a large amount of
133 sequence divergence was previously found between the N2 Bristol and CB4856 Hawaiian
134 lineages (Thompson et al. 2015; Andersen et al. 2012), the increased quality of reference
135 genomes, sequencing technology, and variant detection methods enables the identification of
136 additional variations (in particular large structural variations) that previously went undetected in
137 these *C. elegans* genomes.

138 Recently, Bristol and Hawaiian genomes were reassembled *de novo* using a
139 combination of short-read Illumina sequencing as well as long-read sequencing from PacBio
140 and Oxford Nanopore platforms (Yoshimura et al. 2019; Kim et al. 2019). Compared to the
141 previous short-read based assemblies of N2 Bristol, the new assembly of N2 Bristol, called
142 VC2010, identified 53 more predicted genes, 1.8Mb of additional sequence, and eliminated 98%
143 of existing gaps in the N2 Bristol genome. Thus, the VC2010 Bristol genome very likely better
144 represents the genome of Bristol *C. elegans* currently used in laboratories worldwide

145 (Yoshimura et al. 2019). The first CB4856 Hawaiian genome assembly was completed in 2015
146 by iteratively correcting the pre-existing N2 Bristol reference assembly (*C. elegans* Sequencing
147 Consortium 1998) with short-read sequencing data (Thompson et al. 2015). This study identified
148 327,050 single-nucleotide polymorphisms (SNPs) and nearly 80,000 indels relative to N2; a
149 marked increase relative to previous comparisons, which had identified 6,000-17,000 SNPs and
150 small indels (Wicks et al. 2001; Swan et al. 2002) between N2 Bristol and CB4856 Hawaiian.
151 Due to the size of the short read sequences employed in the analysis, the iterative correction
152 method used to assemble the CB4856 Hawaiian genome may not have detected all structural
153 rearrangements and repetitive sequences. In 2019, the first *de novo* CB4856 Hawaiian
154 assembly from long-read sequencing extended the length of the Hawaiian genome, and was
155 further able to characterize over 3,000 previously uncharacterized SVs (Kim et al. 2019). Thus,
156 combining long-read and short-read sequencing in *de novo* genome assembly not only
157 extended the known length of both the N2 Bristol and CB4856 Hawaiian isolate genomes, but
158 broadened our understanding of how much genomic variation exists between these wild-type
159 strains.

160 Many *C. elegans* research labs utilize N2 Bristol and CB4856 Hawaiian as standard wild
161 type strains, but long-term passaging in each lab may lead to the accumulation of many smaller
162 sequence variants and large genomic structural variations. Early assessments of laboratory
163 lineages of the N2 Bristol strain, for example, identified many duplications ranging in size from
164 200bp to 108kb, with some affecting as many as 26 genes (Vergara et al. 2009). To determine
165 the extent of genetic variation between our laboratory lineages of N2 Bristol and CB4856
166 Hawaiian, we generated two high-quality reference assemblies for the N2 and CB4856 strains
167 used in our laboratory to compare to that of other high-quality reference genomes for N2 and
168 CB4856. By leveraging recent technological advancements in sequencing and variant detection,
169 we provide a comprehensive annotation of SNPs, indels, structural variations, and transposable
170 elements between our lineages of the Bristol and Hawaiian strains. From our comprehensive

171 mapping of TEs in our reference genomes, we report Zator elements to be the most abundant
172 and mobile TE family in the *C. elegans* genome. Further, by comparing our assembled
173 genomes to recently published VC2010 Bristol and CB4856 Hawaiian long-read assemblies
174 (Yoshimura et al. 2019; C. Kim et al. 2019), we identified SNPs, indels, and SVs unique to
175 different lab wild type strains. These variations were enriched in intergenic regions of the *C.*
176 *elegans* genome, suggesting that variations in regulatory sequences and other non-coding
177 regions may underlie the phenotypic variances previously observed between laboratory strains.
178 Taken together, our systematic analysis of genetic variation between natural and laboratory wild
179 type isolates highlights the impact of large structural variants, TE composition, and other
180 chromosomal rearrangements accumulating in the genomes of laboratory model organisms.

181

182 **Results**

183 ***De novo* genome assembly using combined long and short-read sequencing produces 184 high quality genomes**

185 To perform systematic comparisons of multiple wild type genomes from different
186 laboratory isogenic strains, we generated *de novo* assemblies of N2 Bristol and CB4856
187 Hawaiian. The N2 Bristol genome was assembled from PacBio long-reads with 136x coverage
188 producing 121 contigs and a 100.4Mb genome (Figure 1A) The CB4856 Hawaiian genome was
189 generated from PacBio long-reads with 132x coverage from 169 contigs to give a 98.8Mb
190 assembly (Figure 1B). These long-read assemblies were then supplemented with Illumina
191 paired end short-reads with a sequencing depth of 540x and 628x for N2 Bristol and CB4856
192 Hawaiian respectively (Figure 1A-B).

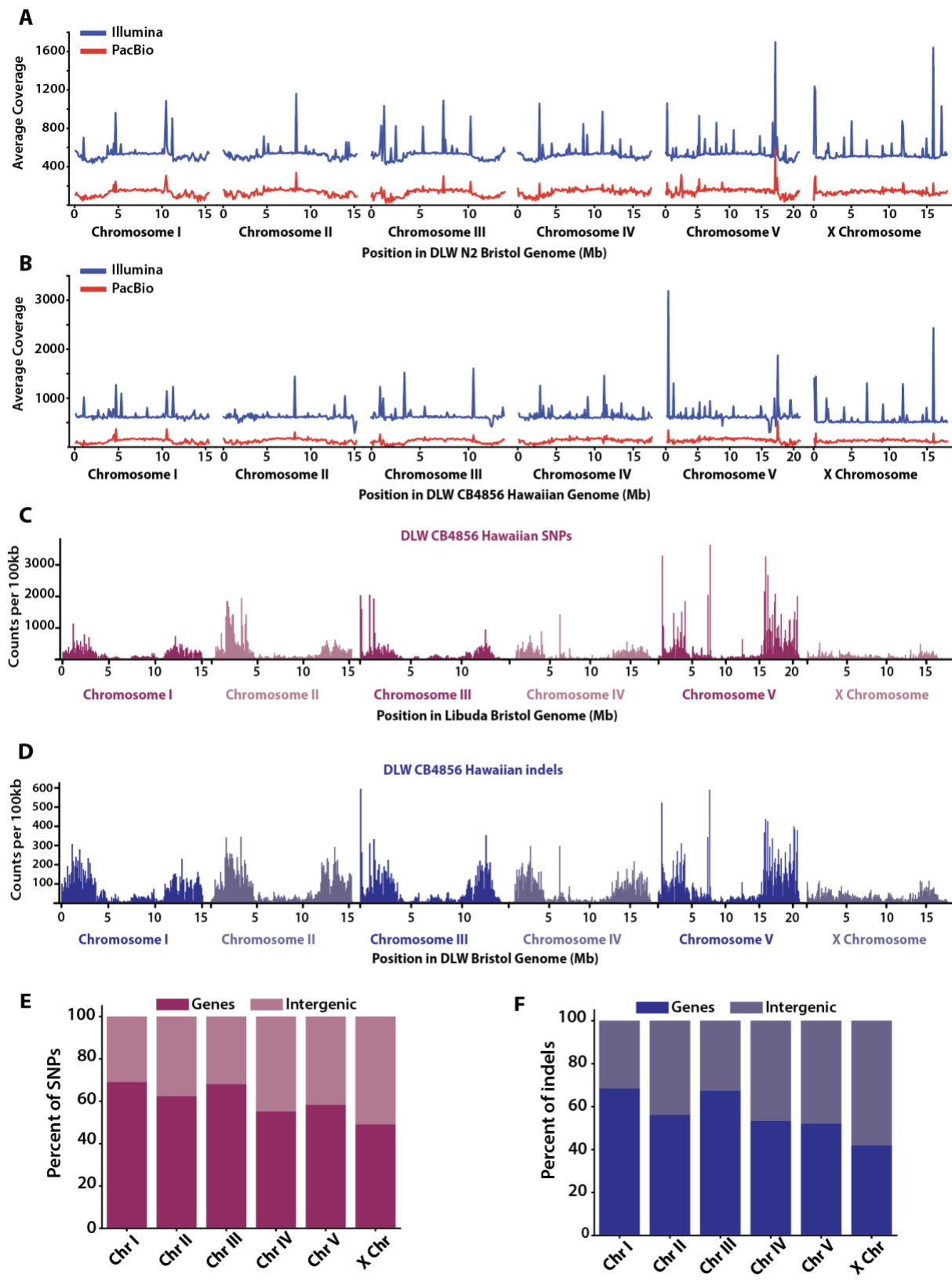
193 To assess the quality of our reference genomes, we examined assembly-to-assembly
194 alignments and the orthologous gene content for each assembly. A strong assembly would
195 show a similar proportion of aligned bases and a high degree of synteny when comparing
196 across assemblies. In concordance with comparisons in earlier studies, 99.2% of bases across

197 our N2 Bristol and CB4856 Hawaiian assembled genomes were aligned (Kim et al. 2019), and
 198 more than 92.2% of bases within alignments were syntenic (Table 1).
 199

Table 1. Comparisons between the DLW N2 Bristol genome (this study) and DLW CB4856 Hawaiian genome (this study)

	Chromosomes						Total
	I	II	III	IV	V	X	
DLW N2 Bristol Chromosome Length (this study)	15,114,068	15,311,845	13,819,453	17,493,838	20,953,657	17,739,129	100,431,990
DLW CB4856 Hawaiian Chromosome Length (this study)	15,045,644	15,257,363	13,206,755	17,183,882	20,547,529	17,584,915	98,826,088
N2 Bristol Bases Aligned	15,100,574	15,303,320	13,222,676	17,330,119	20,947,147	17,738,394	99,642,230 (99.21%)
% Syntenic Aligned Bases	93.31	88.56	90.61	95.42	87.04	98.73	92.23
SNPs*	30,394	48,365	29,881	30,497	87,300	19,861	246,298
Indels*	11,460	13,716	10,530	11,221	20,063	6,799	73,789 (275,442 bp)
SVs	863	808	649	619	925	470	4,334 (2,654,902 bp)
HDRs	185	270	165	138	356	60	1,174 (6,864,884 bp)

200
 201 * All variants listed are only those for which the DLW CB4856 Hawaiian genome was
 202 homozygous



206 **Figure 1. Genomic distribution of SNPs and indels between the DLW N2 Bristol and DLW**
207 **CB4856 Hawaiian genomes. (A)** Line plots showing the average sequencing coverage in
208 100kb bins across each chromosome in the DLW N2 Bristol genome. **(B)** Line plots showing the
209 average sequencing coverage in 100kb bins across each chromosome in the DLW CB4856
210 Hawaiian genome. For each plot in A and B, the coverage for Illumina short-read sequencing is
211 shown in blue, and sequencing coverage for PacBio long-reads is shown in red. **(C)** Histograms
212 depicting the distribution of CB4856 Hawaiian SNPs across each DLW N2 Bristol chromosome
213 in 100kb bins. **(D)** Histograms of the distributions of CB4856 Hawaiian indels across each DLW
214 N2 Bristol chromosome in 100kb bins. **(E)** The proportion of SNPs that overlap with remapped
215 gene annotations versus intergenic regions in the DLW N2 Bristol genome. **(F)** The proportion of
216 indels that overlap with gene versus intergenic regions in the Bristol genome.
217

218 Analysis of universal single-copy orthologs (Simão et al. 2015; Manni et al. 2021) in our *de novo*
219 N2 Bristol and CB4856 Hawaiian genomes revealed greater than 98% completeness
220 (Supplemental Figure S1) and validate that our assemblies are high quality.

221

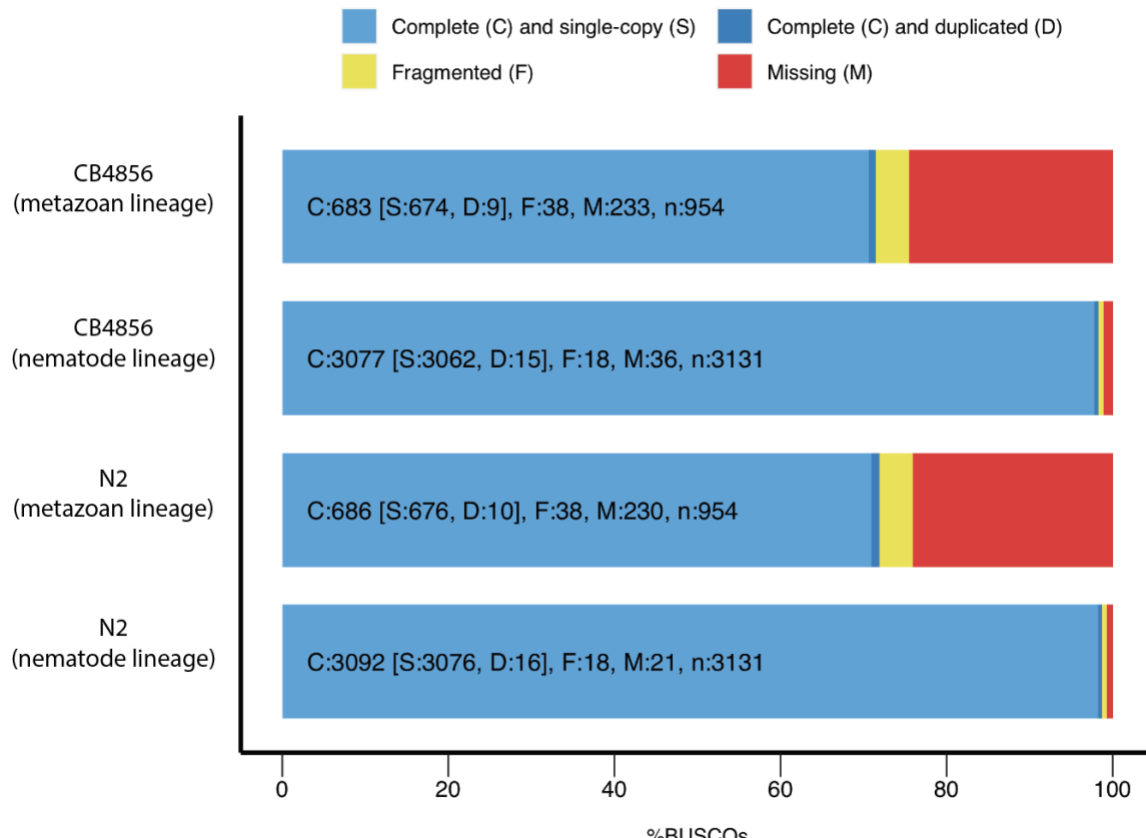
222 ***De novo* genome assemblies of the N2 Bristol and CB4856 Hawaiian isolates enhance**
223 **detection of genomic variation**

224 Previous comparisons of the genetic variation between N2 Bristol and CB4856 Hawaiian
225 have relied on a short-read N2 Bristol reference genome (Thompson et al. 2015; Kim et al.
226 2019), and the amount of variation has yet to be re-assessed using a modern long-read N2
227 Bristol assembly. Utilizing our N2 Bristol and CB4856 Hawaiian strains, we aligned CB4856
228 Hawaiian short reads to our N2 Bristol assembly. This analysis revealed a total of 246,298
229 homozygous SNPs and 73,789 homozygous indels across the genome (Table 1, Figure 1C-D).
230 While many of these SNPs and indels overlapped with gene annotations, they were under-
231 enriched in gene sequences (Figure 1D-E, Supplemental Figure 2). To identify large sequence
232 variants and chromosome rearrangements, we used whole-genome alignments (see Methods).
233 We identified a total of 4,364 structural variants, which are categorized as insertions, deletions,
234 and other chromosomal rearrangements spanning at least 50bp.

235

236

BUSCO Assessment Results

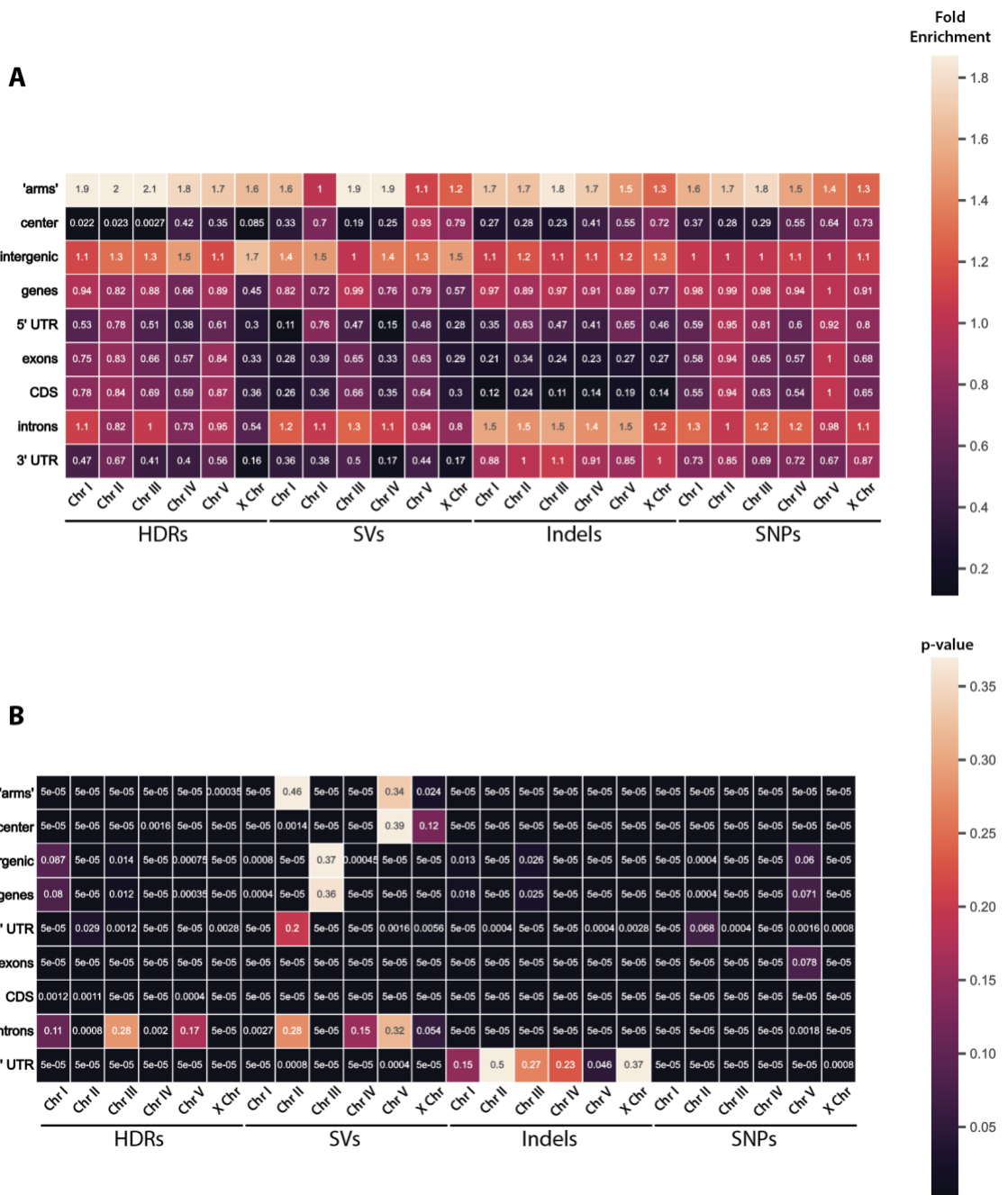


237 **Supplemental Figure S1.** BUSCO analysis of the DLW N2 Bristol and DLW CB4856 Hawaiian
238 genome assemblies. The presence of orthologous genes from metazoan and nematode
239 lineages are shown for each genome assembly. Each orthologous gene analyzed is depicted as
240 either Complete (C, blues), Fragmented (F, yellow), or Missing (M, red). Complete orthologs are
241 then further categorized as single-copy (S, light blue) or duplicated (D, dark blue).
242

243 We also identified 1,174 Highly Divergent Regions (HDRs) (Goel et al. 2019) across the
244 genome. HDRs are defined as regions of the genome over 50bp in length that result in low-
245 quality pairwise alignments due to the presence of multiple gaps within these alignments (Goel
246 et al. 2019). Overall, greater than 9.9% of the DLW N2 Bristol genome (~10.0Mb) displayed
247 variation through SNPs, indels, SVs, and HDRs when compared to the DLW CB4856 Hawaiian
248 genome. SVs and HDRs represented only 1.3% and 0.3%, of variant sites between N2 Bristol
249 and CB4856 Hawaiian respectively, but accounted for over 94% (9.5Mb) of sequence variation
250 (Table1). Including heterozygous variants, our short-read analysis detected 3% more SNPs and

251 18% more indels than previously discovered using short-read assemblies of N2 Bristol and
252 CB4856 Hawaiian (Thompson et al. 2015). Utilizing whole-genome alignment comparisons (Li
253 2018; Goel et al. 2019), we identified 985 more SV sites than previously reported (Nattestad
254 and Schatz 2016; Kim et al. 2019). This increased sensitivity in variant site detection highlights
255 the power of combining long-read and short-read sequencing to create accurate genome
256 assemblies for comparative genomic studies.

257 Given an enhanced detection of variant sites between our N2 Bristol and CB4856
258 Hawaiian assemblies, we were interested in the genome-wide distribution of all variant sites.
259 Given previous reports (Thompson et al. 2015; Kim et al. 2019), we expected a greater density
260 of variation in the terminal thirds (the “arm-like” regions) of each chromosome. Indeed, there is a
261 significant concentration of SNPs, indels, SVs and HDRs in the arm-like regions relative to the
262 central region of each chromosome (Supplemental Figure S2). Over 78% of all SNPs, indels,
263 SVs, and HDRs are in the arm-like domains of each chromosome (Genome-wide averages:
264 75.12% of SNPs, 78.24% of indels, 71.39% of SVs, 90.77% of HDRs). To determine if the
265 enrichment of SNPs, indels, and SVs in the chromosomal arm-like regions was significant, we
266 compared the observed distribution of each variant category with random permutations of each
267 category of variant (Heger et al. 2013). SNPs, indels and HDRs on the autosomes were
268 significantly enriched in the arm-like regions (SNPs: 1.36-1.77 fold enrichment; Indels: 1.47-1.84
269 fold enrichment; HDRs: 1.70-2.06 fold enrichment; $p < 0.001$ by hypergeometric test). SVs,
270 however, were only significantly enriched on the arm-like regions of autosomes I, III, and IV
271 (1.64-1.92 fold enrichment; $p < .001$ by hypergeometric test). The fold enrichment of all variants
272 on the arm-like regions of the X chromosome was slightly weaker, ranging from 1.23-1.64
273 (SNPs: 1.26 fold enrichment; Indels: 1.26 fold enrichment; SVs: 1.23 fold enrichment; HDRs:
274 1.64 fold enrichment; all p -values < 0.05 by hypergeometric test). Similar to previous
275 observations (Thompson et al. 2015), there were a few hyper-variable regions with a greater
276



277 **Supplemental Figure S2.** GAT interval-association test results analyzing the overlap of DLW
278 CB4856 Hawaiian SNPs, indels, and SVs with N2 genome annotations. A) Heatmap showing
279 the fold enrichment of each variant type within gene annotations for each chromosome. B)
280 Heatmap of p-values associated with corresponding fold enrichments shown in panel A
281 calculated by the hypergeometric test.

282

283

284

285

286 density of SNPs and short indels in the central regions of the autosomes, particularly on
287 chromosomes IV and V (Figure 1 C-D).

288
289 Structural variations and HDRs account for most of the base-pairs affected by sequence
290 divergence between our N2 Bristol and CB4856 Hawaiian lineages. The SVs identified ranged
291 in size from 50bp to 592kb (Figure 2D-E), and HDRs ranged from 50bp to 199kb. Within the
292 SVs detected, we identified 47 non-alignable structures, 2 duplications, 18 inversions, and 2
293 translocations. Non-alignable regions (NOTALs) are highly diverged regions containing many
294 repeats and low-complexity sequences that are inhibitory to whole-genome alignment. From our
295 whole-genome alignments of the DLW N2 Bristol and DLW CB4856 Hawaiian genomes, the
296 non-alignable regions between the two genomes comprise 1.39Mb of sequence, ranged in size
297 from 50-592kb, and comprise <0.5% of coding genes in the Bristol genome. One 156kb
298 translocation was found on the right end of CB4856 Hawaiian chromosome V (V:15,871,614-
299 16,027,614bp), while the other translocation, 38kb, was found to be inverted near a telomere of
300 CB4856 Hawaiian chromosome IV (IV: 176:38,447bp). The largest duplication was found on
301 Hawaiian chromosome III (III: 11,819,363-11,860,261). Together, our analyses provide
302 improved variant site identification in wild isolate genomes and further illuminates previously
303 undetected large structural variations and HDRs.

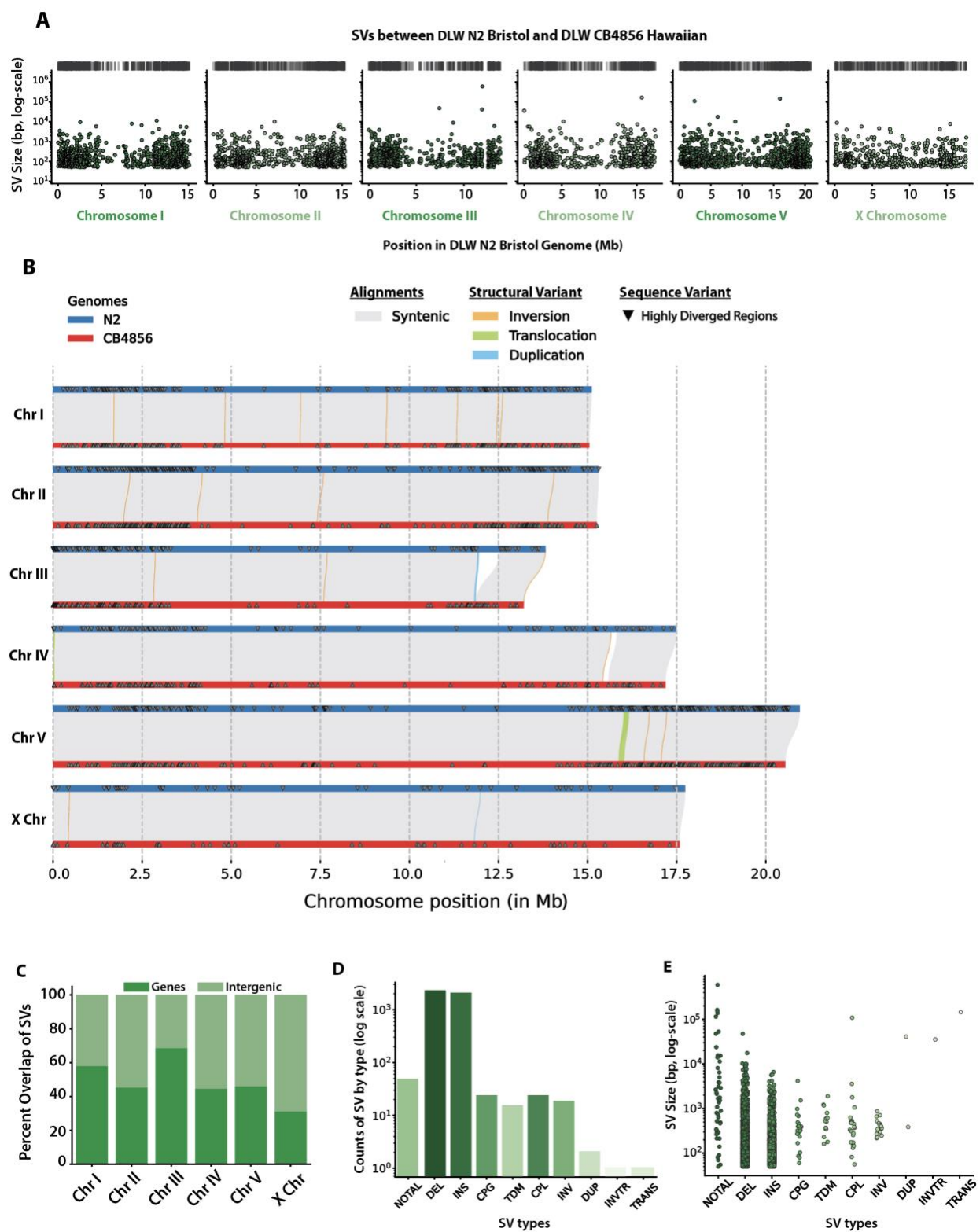
304

305 **SNPs, indels, and SVs are under-enriched in coding regions**

306 Genes are enriched in the central region of all chromosomes in *C. elegans* (*C. elegans*
307 Sequencing Consortium 1998), but there are some genes scattered across the chromosome
308 arm-like regions. While much of the sequence variation is enriched in the arm-like regions, we
309 wanted to know whether this variation was affecting coding sequences across the genome.
310 Thus, we tested whether the SNPs, indels, SVs, and HDRs we identified between our N2 Bristol
311 and CB4856 Hawaiian assemblies were enriched in genes versus intergenic space. Based on

312 our remapped annotations (see Methods, LiftOff (Shumate and Salzberg 2021)), approximately
313 61.8% of the DLW N2 Bristol genome is comprised of gene sequences, with exons and introns
314 representing 28.6% and 33.2% of the genome, respectively. Thus, we would expect
315 corresponding proportions of each variant type to overlap within each annotation if variant sites
316 were uniformly distributed across the genome. To determine if SNPs and indels were enriched
317 in genes, we used the Genomic Association Tester (Heger et al. 2013) to compare the observed
318 overlap of our variant sites in each remapped annotation to simulated uniform distributions of
319 SNP and indel intervals. Fold enrichments represent the ratio of observed overlap to simulated
320 overlaps, whereby a fold enrichment of 1.0 means there is no difference between the observed
321 and simulated datasets. The greatest overlap of SNPs and indels in gene regions were
322 observed on the autosomes (SNPs: 55.2-69.1%; indels: 52.1-68.5%), while only 49.1% of SNPs
323 and 42.0% of indels were found in genes on the X chromosome (Figure 1 E-F). Across the
324 genome, SNPs were slightly under-enriched in gene regions with an average fold enrichment of
325 0.96 (hypergeometric test, p-value <0.05). The average fold enrichment of indels in gene
326 regions was lower than observed with SNPs (fold enrichment of 0.90, p-value <0.05), which
327 could be due to selection against indels within coding regions. For SNPs and indels that did
328 overlap with genes, intron sequences harbored the greatest amount of each variant type (SNPs:
329 fold enrichment 1.14; indels: fold enrichment 1.45; Supplemental Figure 2). In conclusion, SNPs
330 and indels are slightly overrepresented in intergenic regions of the *C. elegans* genome.

331 The distribution of SVs and HDRs across each chromosome resembles the genomic
332 distribution of SNPs and indels (Figure 2A-B). To determine whether these large variant regions
333 were enriched in intergenic versus coding regions, we compared the enrichment of simulated
334 uniform distributions of SVs to those we identified. On the autosomes, 44.5-68.5% of SVs
335 overlapped with gene regions compared 31.1% on the X chromosome (Figure 2C). Compared
336 to SNPs and indels, structural variations on each chromosome, except chromosome III,



339 **Figure 2. Genomic distribution and size of SVs between the DLW N2 Bristol and DLW**
340 **CB4856 Hawaiian genomes.** **(A)** Histograms depicting the distribution of SVs across each
341 chromosome in 100kb bins. Black dashes above each histogram correspond to the genomic
342 locations of SVs that are greater than 20kb in size. **(B)** Chromosome alignment plot depicting
343 syntenic regions between N2 Bristol and CB4856 Hawaiian, structural variants, and highly
344 divergent regions (HDRs). The width of lines showing SVs are proportional to their size. Only
345 rearrangements 1kb or greater in size are shown. **(C)** Stacked bar plots showing the
346 percentage of CB4856 Hawaiian SVs that overlap with intergenic and gene-coding regions of
347 the DLW N2 Bristol genome. **(D)** Bar plots showing the number of each type of SV identified.
348 **(E)** Strip plots showing the log-scaled size distribution of SVs separated by type. For SV types:
349 NOTAL = non-aligned regions, DEL =deletion, INS = insertion, CPG = copy gain in query
350 genome, CPL = copy loss in query genome, TDM = tandem repeat region, INV = inversion,
351 DUP = duplication, TRANS = translocation, and INVTR = inverted translocation. For D and E,
352 different colors only correspond to the different types of SV identified.
353
354

355 displayed significant fold enrichments in intergenic regions (fold enrichments 1.3-1.5, p-values <
356 0.001; Supplementary Figure S2). Similar to SVs, highly divergent regions overlapped with 38.7-
357 66.6% of genes on the autosomes and 24.3% on the X chromosome. HDRs were significantly
358 enriched in intergenic regions of all chromosomes except chromosome I (fold enrichments 1.15-
359 1.65; p-values < .05). Taken together, our data demonstrate that non-coding regions on the
360 chromosome arm-like regions harbor most of the sequence variation between N2 Bristol and
361 CB4856 Hawaiian lineages.

362

363 **Minimal movement of DNA transposons between the N2 Bristol and CB4856 Hawaiian**
364 **lineages**

365 Early analyses of the *C. elegans* genome indicated that approximately 12-16% of the
366 genome is comprised of transposable elements (TEs) (*C. elegans* Sequencing Consortium
367 1998; Bessereau 2006), with *Tc1/mariner* elements as one of the most widely studied DNA
368 transposons that can be active in laboratory strains (Emmons et al. 1983; Liao, Rosenzweig,
369 and Hirsh 1983). While transposable element distributions have been assessed in wild *C.*
370 *elegans* strains using older reference genomes and Illumina short-read sequencing (Laricchia et
371 al. 2017), the complete TE composition has not yet been reassessed in a *de novo* assembly
372 built from long-read sequencing. Further, new families of eukaryotic Class II transposons, have

373 been discovered (Bao et al. 2009), and it remains unclear if these emerging families of DNA
374 transposable elements comprise a significant proportion of the *C. elegans* genome.

375 To identify and locate known transposable element sequences in our N2 Bristol and
376 CB4856 Hawaiian assembled genomes, we used a transposable element identification pipeline
377 that applies an ensemble of programs to find all known RNA and DNA transposable element
378 families (Riehl et al. 2022). We found that approximately 14.7 and 14.3% of our N2 Bristol and
379 CB4856 Hawaiian assemblies, respectively, are composed of transposable element sequences
380 (Supplemental Table 1). For both genome assemblies, the distribution of TEs was concentrated
381 in the terminal third, arm-like regions of each chromosome (Figure 3A-B). Class II DNA TEs
382 represented 96% of all TEs identified in each genome, and Zator elements are 52% of these
383 Class II DNA TEs present in each genome (Supplemental Table 1, Figure 3C-D). To our
384 knowledge, movement of Zator elements and other recently identified TE families has not yet
385 been analyzed in *C. elegans* laboratory strains. Further, we also found that N2 Bristol genome
386 has 20.6% more TEs from the *Tc1/mariner* family than the CB4856 Hawaiian genome
387 (Supplemental Table 1).

388

389

390

391

392

393

394

395

396

397

398

399

400

401

402

403

404

405

406

407 **Supplemental Table 1. Transposable Elements identified in DLW N2 Bristol genome (this**
408 **study) vs DLW CB4856 Hawaiian genome (this study)**
409

	DLW N2 Bristol	DLW CB4856 Hawaiian
Class I Transposable Elements (Retrotransposons)	710 (2,688,730 bp)	776 (2,522,357 bp)
Gypsy	557 (2,195,895 bp)	592 (2,031,038 bp)
Copia	134 (472,195 bp)	161 (465,785 bp)
SINE	9 (2,146 bp)	9 (1,945 bp)
ERV	7 (8,280 bp)	6 (7,569 bp)
LINE	3 (10,214 bp)	8 (16,038 bp)
Class I intrachromosomal transpositions*	0	
Class I interchromosomal transpositions*	0	
Class II Transposable Elements (DNA transposons)	17,682 (12,055,357 bp)	17,310 (11,606,010 bp)
Tc1/Mariner	1870 (1,298,386 bp)	1,550 (1,131,443 bp)
hAT	3,999 (3,988,461 bp)	3,818 (3,725,667 bp)
CMC	1,679 (3,138,647 bp)	2,011 (3,260,455 bp)
Zator	9,159 (3,009,341 bp)	8,980 (2,907,391 bp)
Novosib	46 (12,060 bp)	28 (12,088 bp)
Helitron	39 (368,980 bp)	43 (329,238 bp)
Sola	821 (226,645 bp)	699 (196,797 bp)
MITE	69 (12,837 bp)	181 (42,931 bp)
Class II intrachromosomal transpositions*	38	
Class II interchromosomal transpositions*	9	

410
411 * All TE sequences with predicted transpositions are relative to the DLW N2 Bristol
412 genome
413

414

415

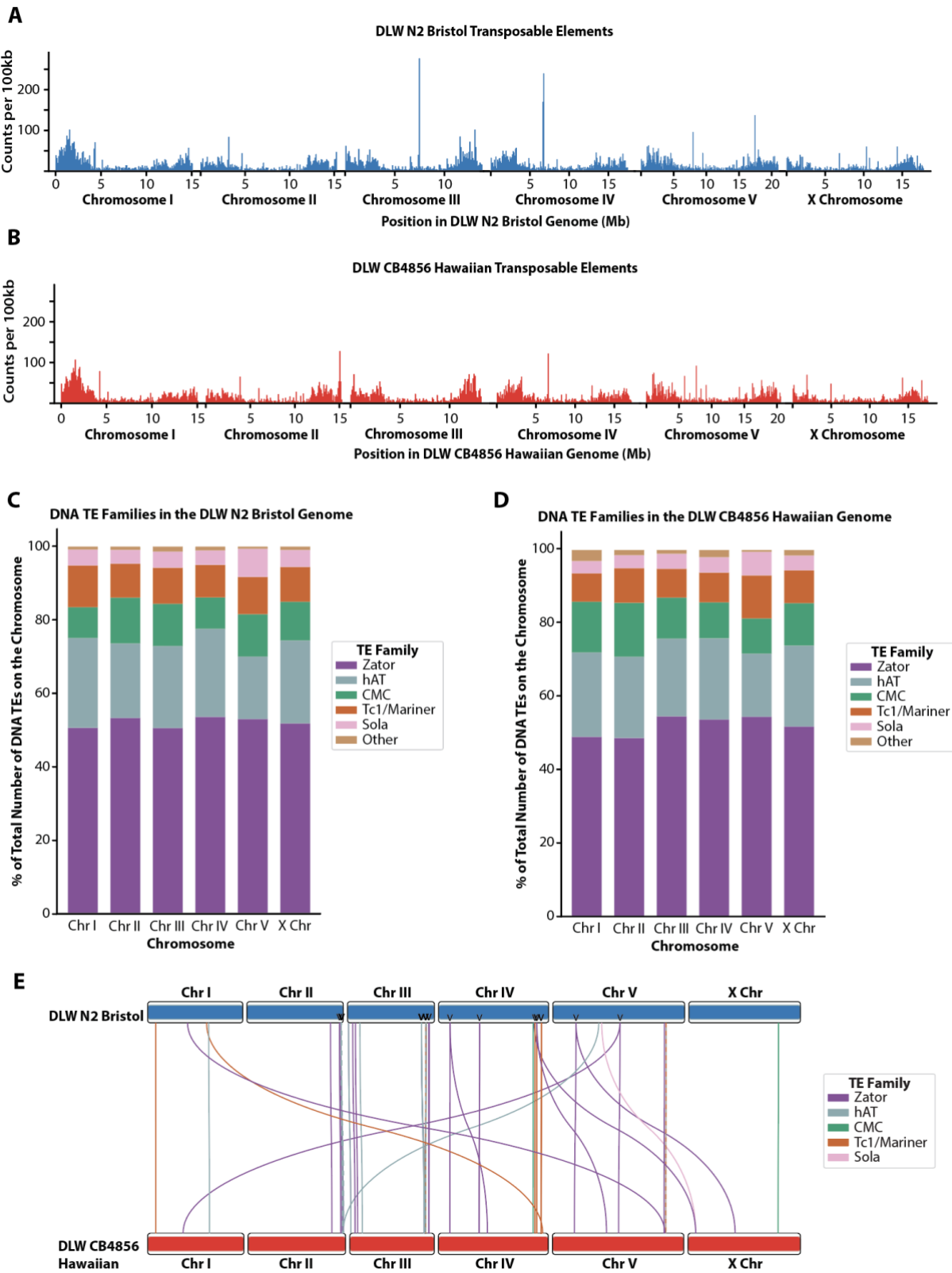
416

417

418

419

420



423 **Figure 3. Genomic distributions of transposable elements in the DLW N2 Bristol and DLW**
424 **CB4856 Hawaiian genomes.** Histograms depicting the distributions of transposable elements
425 across the DLW N2 Bristol genome in 100kb bins. **B)** Histograms depicting the distributions of
426 transposable elements across the DLW CB4856 Hawaiian genome in 100kb bins. **C,D)** Stacked
427 bar plot depicting the percent of total DNA transposable elements on DLW N2 Bristol (C) and
428 DLW CB4856 Hawaiian (D) chromosomes accounted for by specific DNA transposon families.
429 For TE families: CMC= CACTA, Mirage and Chapaev families; hAT = hobo and Activator
430 families; Other = MITE, Novosib and Helitron families. **E)** Ideogram depicting the locations of
431 individual DNA transposable elements that moved between the DLW N2 Bristol genome and the
432 DLW CB4856 Hawaiian genome. DLW N2 Bristol chromosomes are represented by the blue
433 boxes on the top, and DLW CB4856 Hawaiian chromosomes by the red boxes on the bottom.
434 Each line represents an individual transposable element sequence, traced from its position on
435 the DLW N2 Bristol genome to its unique position on the DLW CB4856 Hawaiian genome.
436 Transposable elements predicted to have translocated are colored according to transposon
437 class. Arrow heads across the Bristol N2 chromosomes indicate DNA TEs where duplicated
438 copies are found in the Hawaiian CB4856 genome.
439

440 Since the N2 Bristol and CB4856 Hawaiian lineages were geographically isolated for
441 thousands of generations, we sought to utilize our new TE annotation set to identify individual
442 transposition events that occurred over the course of divergence between the two strains. Using
443 whole-genome alignments and the SNPs we previously defined between these two lineages, we
444 identified specific TE sequences with unique polymorphisms that enables individual transposons
445 to be tracked between the N2 Bristol and CB4856 Hawaiian genome assemblies. Of the 18,392
446 total transposable elements identified in the N2 Bristol genome, 9,377 TEs were uniquely
447 identifiable by sequence polymorphism. Among all N2 Bristol TEs with SNPs, only 1,535
448 elements were detectable in the CB4856 Hawaiian genome. While the vast majority of TEs were
449 found to have not moved within either genome, we did identify 38 Class II DNA TEs that moved
450 intrachromosomally and 9 TEs that moved interchromosomally (Figure 3E). Specifically, we
451 detected 6 Zator elements and one each of *Tc1/mariner*, *Sola*, and *hAT* elements at different
452 interchromosomal locations between the two lineages. In this analysis, we also found several
453 unique copies of Class II DNA transposable elements in the N2 Bristol genome that had
454 duplicated copies in the CB4856 Hawaiian genome (Figure 3E, arrowheads). While we were
455 able to identify transposition events relative to the N2 Bristol genome, we cannot accurately
456 infer the history of each CB4856 Hawaiian copy to determine which resulted from transposition

457 versus duplication. Overall, the landscape of transposable elements remains largely unchanged
458 across the history of divergence between the N2 Bristol and CB4856 Hawaiian lineages.

459

460 **Structural variants predominate the sequence divergence between lab strains**

461 Much of the work exploring *C. elegans* genetic diversity utilizes comparisons of different
462 natural isolates (Koch et al. 2000; Wicks et al. 2001; Thompson et al. 2015; Andersen et al.
463 2012). Work on germline mutation rates in *C. elegans*, however, suggest that considerable
464 genetic variation may have been incurred during the laboratory setting (Denver et al. 2009).
465 Given the rate of mutation accumulation in the germline (2.7×10^{-9} mutations per site per
466 generation (Denver et al. 2009)) and a generation time of approximately three days, each N2
467 lineage alone may have accumulated up to ~1,500 single nucleotide mutations since the 1970s,
468 and nearly 790 potential mutations since the first genome was published in 1998 (C. elegans
469 Sequencing Consortium 1998). Notably, this predicted variation does not include the
470 accumulation of indels and structural variations. Thus, the N2 Bristol and CB4856 Hawaiian
471 genomes present in each lab strain likely carries considerable genomic variation relative to
472 other labs isolates. Previous studies using earlier genome assemblies identified many
473 segmental duplications between lab lineages of wild type strains (Vergara et al. 2009). This
474 variation may underpin phenotypic variation as well as previous work that has shown the
475 lifespans of laboratory N2 Bristol isolates varies between 12-17 days (Gems and Riddle 2000).
476 Taken together, accumulating evidence suggests that inter-lab genetic variation in wild type
477 backgrounds may contribute to differences in experimental outcomes. High-quality lab-specific
478 reference genomes may be an important tool to understand how genetics influences the
479 phenotypes and processes studied by different laboratory groups.

480 To further evaluate the quality and differences of our genome assemblies, we aligned
481 our N2 Bristol genome to the VC2010 Bristol (Yoshimura et al. 2019), as well as aligned our
482 CB4856 Hawaiian genome to the Kim CB4856 Hawaiian genome (Kim et al. 2019). We

483 expected that examining whole-genome alignments to previously validated long-read
484 assemblies would reveal a striking degree of similarity. Comparing our N2 Bristol genome to
485 VC2010, 99.9% of bases were alignable and 99.8% of bases were in syntenic alignments
486 (Table 2). Analysis of our CB4856 Hawaiian genome versus the Kim CB4856 Hawaiian genome
487 showed that 96.1% of bases were alignable, with 92.3% of bases in syntenic alignments (Table
488 3). This high degree of similarity within alignments gives us increased confidence in the quality
489 of our own genome assemblies.

490 To assess how much genetic variation may exist between lab lineages of the most
491 utilized wild-type strain, we first compared our N2 Bristol genome to VC2010 Bristol. We
492 identified 1,162 homozygous SNPs and 1,528 homozygous indels. (Figure 4A-B, Table 2). In
493 total, over 2.07Mb were affected by SNPs, indels and SVs, with 99.7% of this sequence
494 divergence due to structural variations (Figure 4C, Table 2). While highly divergent regions have
495 been observed between wild populations of *C. elegans* (D. Lee et al. 2021), we were also able
496 to identify over 404kb of sequence as HDRs between these two laboratory Bristol lineages
497 (Table 2). These HDRs identified between laboratory strains represent regions with multiple
498 gaps between both genomes within a pairwise alignment in regions of synteny (Goel et al.
499 2019). In addition, we identified two inverted duplications (5.4kb and 12.9kb on chromosomes III
500 and V, respectively) and 39 simple inversions. Four of these inversions are over 29kb in size
501 and account for 11.6% of all structural variation between our N2 Bristol and the VC2010 Bristol
502 genomes. SVs of this nature can be particularly disruptive to genome organization by impairing
503 interactions between regulatory sequences or disrupting gene expression through loss of coding
504 regions (Stranger et al. 2007; Hurles, Dermitzakis, and Tyler-Smith 2008).

505 Examination of our CB4856 Hawaiian lineage compared to the Kim *et al.*, 2019 CB4856
506 Hawaiian assembly (Kim et al. 2019) revealed a greater amount of sequence divergence than
507 comparisons between laboratory lineages of N2 Bristol. We identified 541 homozygous SNPs

508 and 1,298 homozygous indels by aligning our CB4856 Hawaiian short reads to the Kim CB4856
509 Hawaiian genome (Supplementary Figure S3, Table 3, see Methods).

510

511

Table 2. Comparisons between the DLW N2 Bristol genome (this study) and VC2010 Bristol genome

	Chromosomes						Total
	I	II	III	IV	V	X	
DLW N2 Bristol Chromosome Length (this study)	15,114,068	15,311,845	13,819,453	17,493,838	20,953,657	17,739,129	100,431,990 bp
VC2010 Bristol Chromosome Length (Yoshimura et al., 2019)	15,331,301	15,525,148	14,108,536	17,759,200	21,243,235	18,110,855	102,078,275 bp
DLW N2 Bristol Bases Aligned	15,108,942	15,310,622	13,819,294	17,492,076	20,852,291	17,738,432	100,321,657 bp (99.89%)
% Syntenic Aligned Bases	98.83	99.83	99.47	99.12	99.05	99.50	99.28
SNPs*	169	124	164	209	280	216	1,162
Indels*	150	261	210	262	378	267	1,528 (3465 bp)
SVs	113	134	83	228	175	164	897 (2,010,282 bp)
HDRs	8	14	10	21	24	11	88 (406,737 bp)

512

513 * All variants listed are only those for which the VC2010 Bristol genome was homozygous

514

515

516

517

518

519

520

521

522

523

524

525

526

527

528

529

530

531

Table 3. Comparisons between the DLW CB4856 Hawaiian genome (this study) and Kim CB4856 Hawaiian genome

	Chromosomes						Total
	I	II	III	IV	V	X	
DLW CB4856 Hawaiian Chromosome Length (this study)	15,045,644	15,257,363	13,206,755	17,183,882	20,547,529	17,584,915	98,826,088
Kim CB4856 Hawaiian Chromosome Length (Kim et al., 2019)	15,528,896	15,813,191	14,110,336	17,985,219	21,389,866	18,073,349	102,900,857
DLW CB4856 Hawaiian Bases Aligned	14,620,886	14,680,704	12,451,582	16,482,840	19,427,050	17,371,269	95,034,331 (96.16%)
% Syntenic Aligned Bases	94.91	92.38	93.01	89.28	89.24	96.10	92.32
SNPs*	60	52	71	108	135	115	541
Indels*	240	190	175	242	238	213	1,298 (2157 bp)
SVs	148	274	194	626	660	168	2,070 (6,923,335 bp)
HDRs	19	70	25	100	144	12	370 (3,327,407 bp)

532

533 * All variants listed are only those for which the Kim CB4856 Hawaiian genome was
534 homozygous

535

536 Notably, analysis of our whole-genome alignments identified over 9.5Mb of structural variation

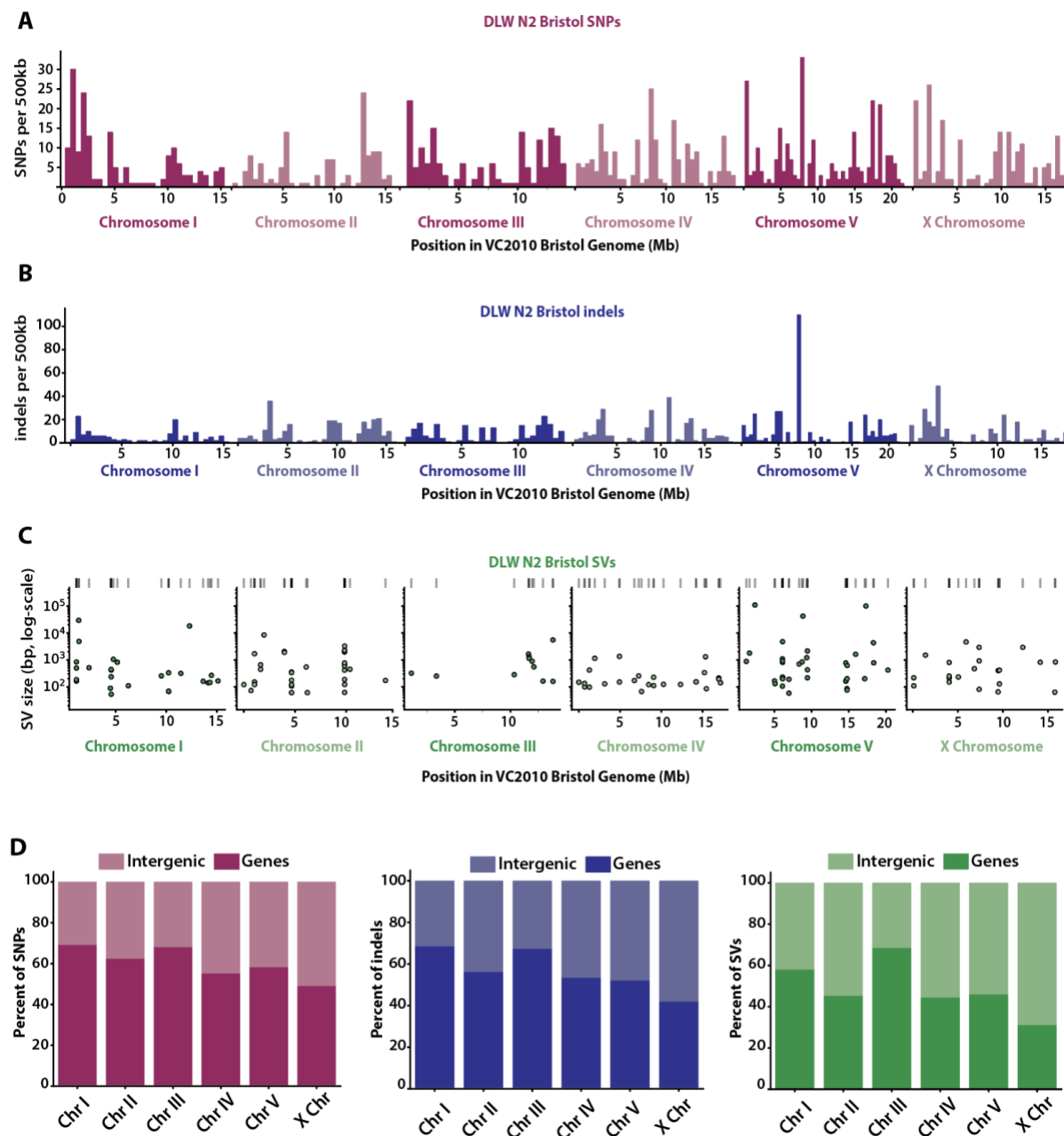
537 and HDRs between these two genomes. More than 66% of this structural variation, however, is

538 due to unique, non-alignable regions. These non-alignable regions are highly divergent with

539 many gaps in pairwise alignments that contain many repeats and low-complexity sequences.

540 Further, over 3.3Mb in each Hawaiian genome falls within highly divergent regions. Taken

541 together, we detected much more variation than anticipated between laboratory wild-type
542 genomes. In the laboratory isolates of N2 Bristol and CB4856 Hawaiian, SVs affected the
543 greatest number of base pairs, with a large portion of this variation due to large non-alignable



544

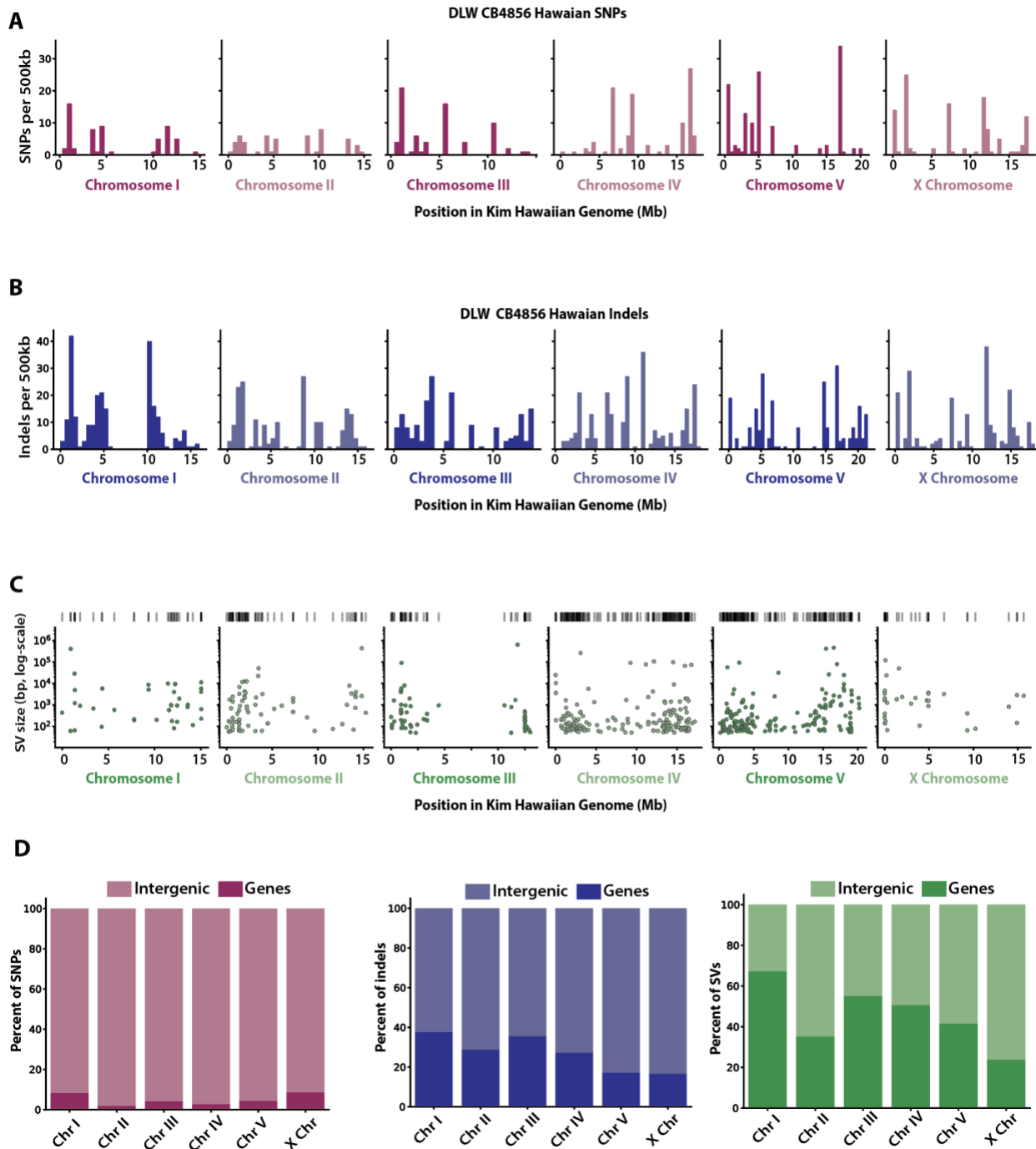
545 **Figure 4. Genomic variation between the DLW N2 Bristol genome and the VC2010 Bristol**
546 **genome. (A-B)** Histograms depicting the distribution of DLW N2 Bristol SNPs and indels across

547 each VC2010 Bristol chromosome in 500kb bins. **(C)** Scatterplots showing the genomic position

548 of SVs with the log-scaled size of each SV on the y-axis. **(D)** The proportions of DLW N2 Bristol

549 SNPs, indels, and SVs that overlap with intergenic versus gene-coding regions of the VC2010
 550 Bristol genome.
 551

552



553

554 **Supplementary Figure S3.** Genomic variation between the DLW CB4856 Hawaiian genome
555 and the Kim CB4856 Hawaiian genome. (A-B) Histograms depicting the distribution of SNPs
556 and indels across each Kim CB4856 Hawaiian chromosome in 500kb bins. (C) Scatterplots
557 showing the genomic position of SVs with the log-scaled size of each SV on the y-axis. (D) The
558 proportions of DLW CB4856 Hawaiian SNPs, indels, and SVs that overlap with intergenic
559 versus gene-coding regions of the Kim CB4856 Hawaiian genome.
560

561 regions, duplications, and inversions. Thus, the genomes of wild type strains present in some
562 labs are not only unlike the most widely used reference genome in the *C. elegans* research
563 community, but there are likely many large inter-lab genomic variations that might underlie some
564 of the phenotypic differences observed in laboratory strains.

565

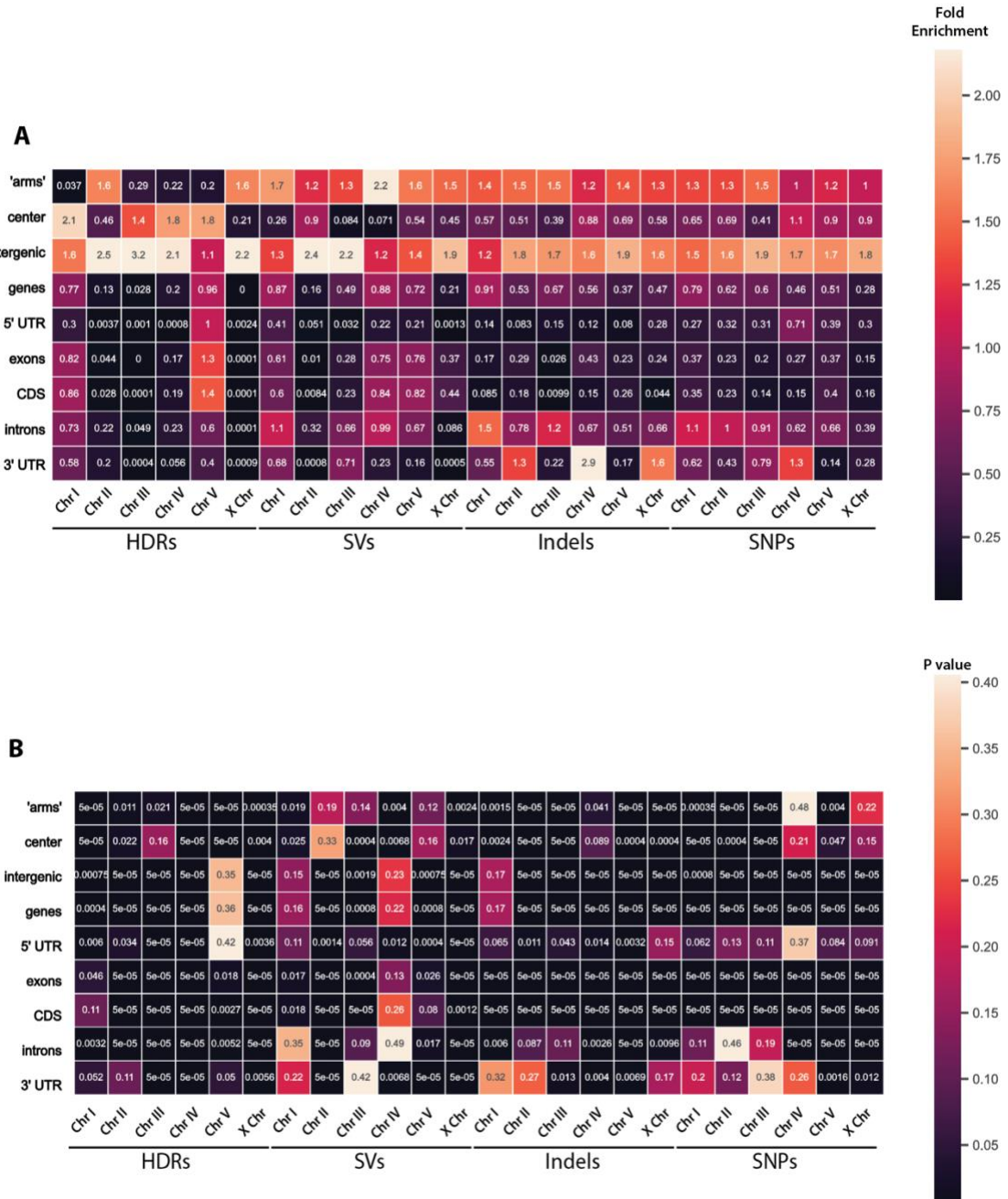
566 **Intergenic enrichment of variant sites between lab lineages of N2 Bristol and CB4856
567 Hawaiian**

568 To determine whether specific genomic regions of lab strains are susceptible to
569 sequence variation, we repeated our analysis of the genomic distributions of each variant class
570 and assessed the enrichment of variant sites in gene annotations. We used LiftOff to remap the
571 pre-existing Bristol gene annotations onto both the VC2010 Bristol and Kim CB4856 Hawaiian
572 assemblies with similar success. To address whether the sequence divergence is nonrandomly
573 enriched in each region of interest, we again used GAT to simulate random SNP, indel, SV, and
574 HDR intervals 20,000 times and compared the simulated overlap to what we observed in
575 between genomes. Notably, the stereotypical “arms”-vs-“center” genomic distribution of variants
576 seen when comparing Bristol and Hawaiian genomes is not true for all chromosomes when
577 comparing our Bristol genome to VC2010 (Figure 4A-C), with some chromosomes displaying a
578 concentration of variation in the central region. SNPs were 1.2-1.5 fold enriched in the arm-like
579 regions of chromosomes I, II, III, and V (p-values <0.01). Indels, however, were concentrated in
580 the arm-like regions of all chromosomes with fold enrichments ranging from 1.2-1.5 (p-values <
581 0.05). While SVs were 1.2-2.2 fold enriched in the arm-like regions of each chromosome, this
582 enrichment was only significantly higher than expected by null distributions on chromosomes I,

583 IV, and the X chromosome (Supplemental Figure S4). Further, HDRs between Bristol lineages
584 were 1.6 fold enriched on the arm-like regions of chromosome II and the X chromosome (p-
585 values < 0.05), while displaying significant 1.8-2.1 fold enrichments in the center regions of
586 chromosomes I, IV, and V (p-values < 0.01). Finally, we also wanted to determine whether the
587 variant sites we detected between lab strains impacted gene coding regions. Between the two
588 Bristol lineages, SNPs, indels, SVs, and HDRs were all under-enriched in gene coding regions
589 and displayed significant enrichments in intergenic regions on most chromosomes
590 (Supplemental Figure S4). Thus, variation between laboratory Bristol lineages is largely
591 concentrated in non-coding regions of each chromosome.

592 We next examined the genomic distribution and enrichment of variant sites in gene
593 annotations of the two Hawaiian genomes to see if the patterns of enrichment were similar to
594 the Bristol genomes. After examining the enrichment of all variant types in both the arm-like
595 regions and “centers” of each chromosome, it was clear that most chromosomes were enriched
596 for variant sites in the arm-like regions and intergenic sequences, with a few exceptions as
597 follows. (Supplemental Figure S5). SNPs were only enriched 0.84 fold in the arm-like regions of
598 the X chromosome, and indels were enriched 0.81 fold in the arm-like regions of chromosome
599 IV (p-values < 0.05). SVs were 0.64 fold enriched in the arm-like regions of chromosome II, and
600 HDRs were 0.12 fold enriched in the arm-like regions of chromosome I (p-values < 0.001). We
601 then examined the enrichment of all variants in intergenic versus gene sequences between the
602 two CB4856 genomes. SNPs and indels showed significant 1.7-2.8 fold enrichments in
603 intergenic regions on all chromosomes (p-values < 0.001). SVs displayed a significant 1.2-1.7
604 fold enrichment in the intergenic regions of all chromosomes. HDRs were 1.2-1.7 fold enriched
605 in the intergenic regions of chromosomes II, III, IV, V and the X chromosome (all p-values <
606 0.05). In conclusion, analysis of the genetic variation between respective lab lineages of N2
607 Bristol and CB4856 Hawaiian revealed a striking amount of variation often present in intergenic

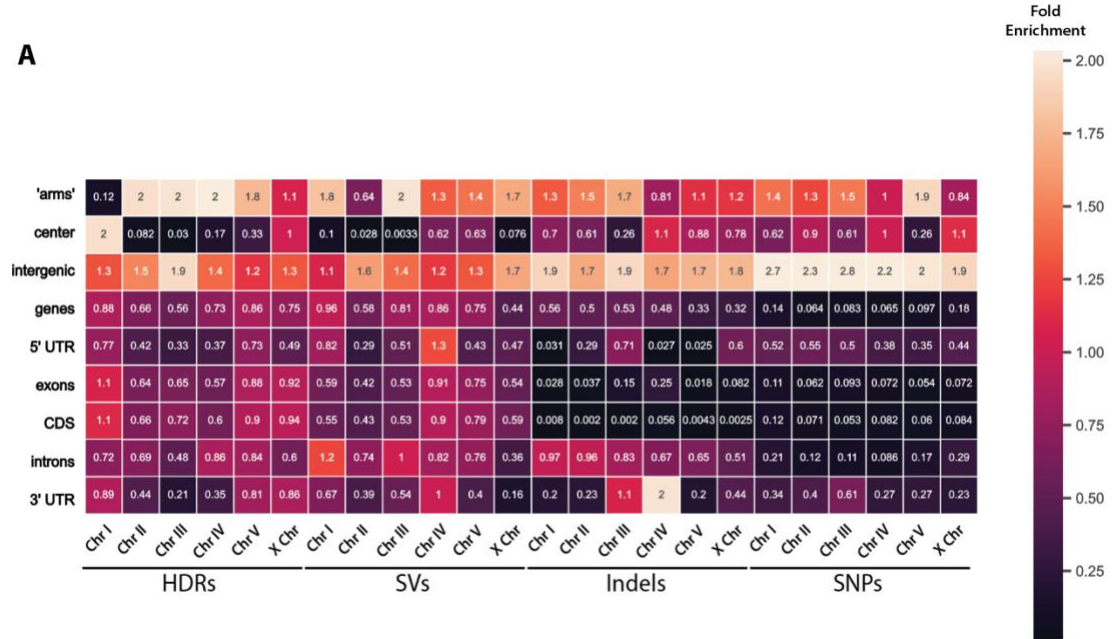
608 sequences, with some weak enrichments in the arm-like regions versus the central regions of
 609 chromosomes.
 610



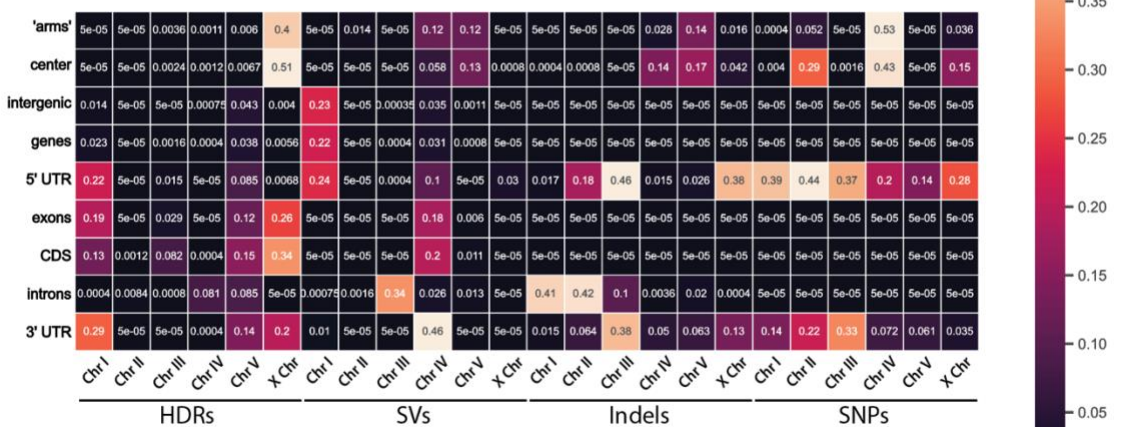
611
 612 **Supplemental Figure S4.** GAT interval-association test results analyzing the overlap of DLW
 613 N2 Bristol SNPs, indels, and SVs with remapped VC2010 Bristol genome annotations. A)
 614 Heatmap showing the fold enrichment of each variant type within gene annotations for each

615 chromosome. B) Heatmap of p-values associated with corresponding fold enrichments shown in
 616 panel A calculated by the hypergeometric test.

A



B



617

618 **Supplemental Figure S5.** GAT interval-association test results analyzing the overlap of DLW
 619 CB4856 Hawaiian SNPs, indels, and SVs with remapped Kim CB4856 Hawaiian genome
 620 annotations. A) Heatmap showing the fold enrichment of each variant type within gene
 621 annotations for each chromosome. B) Heatmap of p-values associated with corresponding fold
 622 enrichments shown in panel A calculated by the hypergeometric test.

623

624

625 **Discussion**

626 Detection and characterization of sequence variation between individuals or across
627 species is fundamental to our functional understanding of genomic elements and consequences
628 of variation. Since the first draft of the *C. elegans* genome was released in 1998, the highly
629 divergent strains N2 Bristol and CB4856 Hawaiian have been used extensively for comparative
630 genomics studies(C. elegans Sequencing Consortium 1998; Koch et al. 2000; Wicks et al. 2001;
631 Maydan et al. 2010; Andersen et al. 2012; D. Lee et al. 2021). The combined usage of short and
632 long read sequencing to assemble genomes and to compare them has both increased the
633 quality of our reference genomes as well as enhanced the genome-wide detection of sequence
634 variants, new genes, and new genomic regions (Yoshimura et al. 2019; C. Kim et al. 2019; B. Y.
635 Kim et al. 2021; Sarsani et al. 2019). In this study, we generate *de novo* assemblies for the N2
636 Bristol and CB4856 Hawaiian *C. elegans* isolates from our lab lineage using short-read and
637 long-read sequencing. Our examination of the inter-lab genetic drift among wild-type strains
638 suggests genomic analyses can be improved by resequencing the genomes of labs' wild-type
639 strains or utilizing strains with recently published, accurate genome assemblies. This also
640 presents a strong argument for labs utilizing *C. elegans* in their research to frequently return to
641 cryogenically preserved stocks of their wild type strains. These genomes will serve as additional
642 tools for future comparative genomics studies, especially in the functional characterization of
643 structural variations identified through whole-genome alignments.

644

645 **Genome assembly and genomic divergence in laboratory isolates**

646 Earlier studies uncovering phenotypic and genetic variations between lab wild-type
647 strains indicated that there are likely many underlying large-scale genomic differences (Denver
648 et al. 2009; Vergara et al. 2009; Gems and Riddle 2000). Here we identify numerous SNPs,
649 indels, SVs, and HDRs between different lab lineages of each wild isolate. The total amount of

650 genomic variation is at levels higher than predicted by earlier mutation accumulation studies.
651 Much of this variation, however, is due to SVs and HDRs, which have only recently become a
652 detailed subject of study (Thompson et al. 2015; Kim et al. 2019; Lee et al. 2021). Our genome
653 assemblies of the Bristol and Hawaiian strains corroborate prior results indicating that genomic
654 variation is enriched in the distal arm-like regions of chromosomes between these natural
655 isolates. Evolutionary genomic analysis has shown that recombination in the arm-like regions of
656 each chromosome and balancing selection likely have shaped this landscape of sequence
657 divergence across the 30,000-50,000 generations these strains have been geographically
658 isolated (Thomas et al. 2015; Kern and Hahn 2018). In contrast, we find that the distribution of
659 variant sites across the arm-like regions versus center domains of each chromosome between
660 lab lineages is not as strong or consistent as seen when comparing N2 Bristol to CB4856
661 Hawaiian genomes. This result could indicate that in relatively short timescales (~3,000-5,800
662 generations), selection for the accumulation of mutations in the arm-like regions, particularly in
663 noncoding regions, is not sufficient to consistently eliminate sequence divergence away from
664 the gene-dense chromosome centers. Further, we found that SNPs, indels, and structural
665 variations were highly enriched in intergenic regions when comparing the genomes of laboratory
666 strains. Although many of the sequence variants we identified are not directly disrupting coding
667 sequences, it remains possible that genetic drift in these regions are altering the function of
668 intergenic regulatory sequences such as promoters and enhancers. Thus, the accumulation of
669 disruptive genomic changes within regulatory regions in the gene-dense centers of
670 chromosomes may underpin many of the phenotypic differences observed in laboratory wild-
671 type strains, such as variance in lifespan (Gems and Riddle 2000).

672

673 **Highly variable arm-like domains on *C. elegans* chromosomes**

674 The arm-like regions of *C. elegans* chromosomes exhibit a striking degree of variation
675 that is highly correlated with large domains of increased recombination, which is a pattern

676 observed in many species (Andersen et al. 2012; D. Lee et al. 2021; Kern and Hahn 2018;
677 Rockman and Kruglyak 2009). In *C. elegans*, these divergent autosomal arm-like domains
678 coincide with a disproportionate fraction of newer, rapidly evolving genes as compared to the
679 center regions of each chromosome, which house highly conserved essential genes (*C. elegans*
680 Sequencing Consortium 1998; Kamath et al. 2003). The development of new tools to detect
681 larger structural variations through alignment of assemblies or long sequencing reads has
682 revealed many SVs on the chromosomal arm-like domains (Mahmoud et al. 2019; C. Kim et al.
683 2019). The fact that SVs are enriched in the arm-like regions, which also display elevated levels
684 of recombination, is notable given the fact that large structural variants such as inversion are
685 typically inhibitory to recombination (Miller, Cook, and Hawley 2019). The arm-like regions of *C.*
686 *elegans* chromosomes are enriched for many repetitive elements, including transposable
687 elements, tandem repeats, and low complexity repeat sequences (*C. elegans* Sequencing
688 Consortium 1998; Surzycki and Belknap 2000). The presence of many SVs in the arm-like
689 regions could be due to errors in double-strand DNA break repair and heterologous
690 recombination in regions adjacent to highly repetitive sequences, thereby causing chromosomal
691 rearrangements. Similar rearrangement events are known to contribute to many human
692 genomic disorders like Prader-Willy Syndrome or Charcot-Marie-Tooth disease (Carvalho and
693 Lupski 2016; Stankiewicz and Lupski 2010). Future investigations assessing the occurrence of
694 SVs adjacent to highly repetitive regions and sites of homologous recombination will be
695 invaluable in understanding how differences in genomic organization arise between divergent
696 lineages of *C. elegans*.

697 With regard to genomic rearrangements and their impact on genome function, renewed
698 attention must be given to the contribution of transposable elements and their mobility within
699 and between chromosomes. While Sola and Zator elements are relatively recent in their
700 discovery within *C. elegans* and other eukaryotic genomes (Bao et al. 2009; Riehl et al. 2022),
701 our data suggests there may be many active TE copies in these families, particularly Zator

702 elements. Historically, much attention has been given to the impact of *Tc1/Mariner* transposition
703 on genomic architecture, but the contribution of Zator elements to changes in genome structure
704 and gene regulation merits further future investigation. Our analysis of TE mobility only
705 examines two endpoints across the long period of divergence between the Bristol and Hawaiian
706 lineages. It remains unclear, however, whether many of these newly characterized TEs remain
707 active and whether they contribute to the growing catalog phenotypic differences displayed
708 between laboratory lineages of Bristol and Hawaiian *C. elegans*.

709
710 Finally, the generation of multiple independent long read *de novo* genome assemblies
711 for both N2 Bristol and CB4856 Hawaiian isolates provides a powerful toolkit for comparative
712 genomics and evolution studies. Many prior studies assessing the *C. elegans* recombination
713 landscape have relied on mapping recombination in worms heterozygous for Bristol and
714 Hawaiian chromosomes. The high sequence divergence and large structural variations between
715 Bristol and Hawaiian which we describe, however, may have positional impact on the
716 distributions of crossover sites. Our identification of variants in Bristol strains enables
717 polymorphism mapping by crossing different lab-lineages of N2 Bristol, avoiding the potential
718 confounding effects of crosses with other wild isolates. Additionally, further identification and
719 functional characterization of polymorphic sites and structural variations present between lab
720 lineages of N2 Bristol and CB4856 Hawaiian could provide new insights into how pronounced
721 phenotypic differences in the lifespan, feeding behavior, and reproductive fitness arise in
722 modern lab-derived strains (Gems and Riddle 2000; Zhao et al. 2018). To summarize, we
723 demonstrate the importance of using long and short-read sequencing to generate modern
724 reference genome assemblies and maximally detect sequence variation, while highlighting the
725 potential genomic underpinnings of phenotypic variations in laboratory lineages of *C. elegans*.

726

727

728 **Methods**

729 ***C. elegans* culture and sucrose floatation**

730 The N2 Bristol and CB4856 Hawaiian strains of *C. elegans* were grown at 20°C on standard
731 NGM agar plates seeded with the OP50 strain of *E. coli* as a food source. To minimize bacterial
732 contamination in downstream gDNA sample preps, we performed sucrose floatation on pooled
733 populations of each isolate. Worms were washed from plates with 8mL cold M9 buffer and
734 transferred to 15mL glass centrifuge tubes using a glass Pasteur pipette. Collected worms were
735 centrifuged at 3000rpm at 4°C and washed in 4mL of fresh M9 twice. To separate worms from
736 bacteria and other debris, 4mL of 60% sucrose solution was added to 4mL of M9 buffer and
737 worms and vortexed briefly. The mixture was then spun at 5000 rpm at 4°C for 5 minutes. Using
738 a glass pipette, the floating layer of worms were transferred to a new glass centrifuge tube on
739 ice and brought up to 4mL in fresh M9. Worms were then incubated at room temp for 30
740 minutes and gently vortexed every 5 minutes. Worms were washed three times in equal volume
741 of fresh M9 were performed before storing collected worms in M9 at 20°C before genomic DNA
742 (gDNA) extraction.

743

744 **Long-read and short-read sequencing**

745 Genomic DNA was extracted from worms using the Qiagen DNeasy Blood and Tissue Kit.
746 Sequencing was performed on pooled populations of N2 and CB4856 after reducing bacterial
747 contamination by sucrose float for each strain. For PacBio long-read sequencing, library
748 preparation was performed on pooled populations of worms for each isolate by the University of
749 Oregon's Genomics and Cell Characterization Core Facility and sequenced on the Sequel II
750 system. For Illumina short-read sequencing, library preparation was performed on pooled
751 populations of worms for each isolate by the University of Oregon's Genomics and Cell
752 Characterization Core Facility. The short-read libraries were then sequenced on an Illumina
753 HiSeq4000 (2 x 150bp).

754

755 **Long-read genome assembly and short-read refinement**

756 PacBio long-reads were aligned to the *E. coli* genome using BWA (Li and Durbin 2009) (version
757 0.7.17), and reads that aligned to the bacterial genome were removed. De novo genome
758 assembly was performed for N2 Bristol and CB4856 Hawaiian using Canu (Koren et al. 2017)
759 (version 1.7). To refine the long-read assemblies, short-reads from each isolate were aligned to
760 their respective long-read assembly using BWA-MEM (version 0.7.17). Aligned reads in SAM
761 format were sorted and converted to BAM format using SAMtools (Li et al. 2009). Using Picard
762 (<https://broadinstitute.github.io/picard/>), read groups were added via
763 AddOrReplaceReadGroups, and duplicate reads were filtered using MarkDuplicates. Some
764 bases may have been inaccurately called due to lower sequencing coverage, larger error rate in
765 PacBio sequencing, or predominating alleles present in the population of each isolate that could
766 be revealed by greater sequencing depth afforded by Illumina sequencing. GATK's
767 HaplotypeCaller (McKenna et al. 2010) and Freebayes (Garrison and Marth 2012) were utilized
768 to generate VCF files representing potentially inaccurate sites in each initial assembly.
769 Coverage thresholds were manually determined using IGV for each assembly. Sites were
770 filtered according to manual values using VCFtools (Danecek et al. 2011; Danecek and
771 McCarthy 2017)). Error correction was performed on single-nucleotide alleles using BCFtools
772 *consensus* (Danecek and McCarthy 2017) and alternate indel alleles. After filtering potential
773 sites by sequencing depth thresholds determined for each chromosome, this left 4237 and
774 36145 corrections for the N2 Bristol and CB4856 Hawaiian genomes, respectively. Of these
775 sites, less than .7% were unable to be resolved, and all of these were short indels comprising
776 less than .001% of each genome.

777

778 **Assessing genome assembly completeness**

779 To further assess the quality and completeness of our N2 Bristol and CB4856 Hawaiian
780 assemblies, we used BUSCO (Simão et al. 2015; Manni et al. 2021). BUSCO was run in a
781 Docker container (https://busco.ezlab.org/busco_userguide.html) in genome mode. For each
782 assembly, the quality and presence of expected orthologous genes was checked against the
783 nematoda and metazoan lineage databases.

784

785 **SNP and indel Calling in N2 and CB4856 assemblies**

786 Illumina short reads from the DLW N2 Bristol and DLW CB4856 Hawaiian genome were
787 trimmed using Trimmomatic (Bolger, Lohse, and Usadel 2014) to remove adapter and barcode
788 sequences. The trimmed CB4856 reads were then aligned to the DLW N2 Bristol reference
789 genome using BWA-MEM so that SNPs and indels present between N2 Bristol and CB4856
790 Hawaiian could be identified. All resulting variant positions comparing our N2 Bristol and
791 CB4856 Hawaiian genomes are in relation to the N2 Bristol assembly. Aligned reads in SAM
792 format were then sorted using SAMtools (Li et al. 2009) and converted to BAM files. Using
793 Picard read groups were added via AddOrReplaceReadGroups, and duplicate reads were
794 filtered using MarkDuplicates as described above. BAM files with filtered duplicate reads were
795 used to call variants using a combination of GATK HaplotypeCaller, Freebayes, and BCFtools.
796 The three resulting VCF files containing SNPs and indels were then concatenated, further
797 filtered for duplicate sites and low-quality variants, and sorted using BCFtools. SNPs with QUAL
798 scores of 30 or greater, a minimum of 10 variant reads, and a minimum of 30 total, high-quality
799 reads were retained. To draw comparisons between other N2 assemblies, the most recent gene
800 annotations were downloaded from WormBase (*C. elegans* VC2010, PRJEB28388). For
801 comparisons between CB4856 Hawaiian genomes, assemblies were downloaded WormBase
802 (*C. elegans* CB4856, PRJNA275000) and the NCBI BioProject Database under accession
803 number PRJNA523481. To call variants between our N2 Bristol and CB4856 Hawaiian

804 assemblies and those generated by other labs, short reads were aligned to the respective
805 genomes and the SNP and indel calling pipeline was repeated as described above.

806

807 **Calling Structural Variants using whole-genome alignments**

808 All assembly-to-assembly alignments were performed using Minimap2 (Li 2018). SyRI (Goel et
809 al. 2019) was then used to parse the resulting SAM files and call structural variants and highly
810 divergent regions (Structural rearrangements were plotted with the aid of Plotsr within the SyRI
811 package. “NOTAL” or non-alignable regions in each genome were retained as SVs. To acquire
812 NOTAL regions in each query genome, the Minimap2 alignment was repeated with the original
813 reference and query genomes swapped. The sizes of HDRs depicted in Tables 1-3 are sizes
814 relative to the reference genome in each comparison (*i.e.* N2 Bristol in Table 1). When
815 comparing our CB4856 Hawaiian genome to the Kim CB4856 genome, 89% of the size
816 difference in assemblies can be accounted for in the net sequence gained from Kim HDRs and
817 unique NOTAL structures. NOTAL structures and gap-adjacent sequences in the Kim CB4856
818 genome are 1.5 and 1.6-fold enriched for low complexity and repeat sequences, respectively.
819 These regions and sequence features are challenging for genome assembly and likely explain
820 megabase-scale differences in genome assembly sizes.

821

822 **Converting gene annotations between assemblies**

823 We converted gene annotations from the N2 reference assembly (cel235) to our N2 Bristol and
824 CB4856 Hawaiian assemblies, as well as the VC2010 Bristol and Kim CB4856 Hawaiian
825 assemblies. The gene annotations for the WBcel235 genome assembly were downloaded in
826 GFF3 format from Ensembl (http://ftp.ensembl.org/pub/release-105/gff3/caenorhabditis_elegans/). Unlike previously established tools that require pre-
827 generated chain files (James et al. 2003), Liftoff (Shumate and Salzberg 2021) can accurately
828 remap gene annotations onto newly generated assemblies using Minimap2 assembly-to-

830 assembly alignments. Rather than aligning whole genomes, Liftoff aligns only regions listed in
831 the annotation files so that genes may be remapped even if there are large structural variations
832 between two genomes. The Liftoff program was then used to remap annotations between the
833 WBcel235 assembly onto each new genome assembly for N2 Bristol and CB4856 Hawaiian).

834

835 **Testing the association between variant sites and gene annotations**

836 For each chromosome, to determine whether SNPs or indels were enriched within gene
837 annotations, fold enrichment analyses were performed using the genomic association tester
838 (GAT) (Heger et al. 2013) tool (<https://github.com/AndreasHeger/gat.git>). The observed
839 enrichment of each variant type in gene annotations was compared to overlaps in simulated
840 distributions SNPs or indels. Simulated distributions were created using 20,000 iterations
841 whereby each variant type was randomly and uniformly distributed across each chromosome.
842 SNPs and indel distributions were compared against intergenic, gene, intron, exon, and UTR
843 annotations. Comparing the observed enrichment to the simulated distributions, statistical
844 significance was assigned to the observed fold enrichment with p-values calculated from a
845 hypergeometric test calculated within GAT. Per-chromosome BED files for SNP intervals were
846 created from their original VCF using AWK. Per-chromosome BED files for indel intervals were
847 calculated using a custom script. The GFF3 formatted annotations generated via liftoff were
848 then broken down by chromosome, gene, exon, and UTR regions. Because intron regions were
849 not explicitly written into each GFF3 file, they were calculated using BEDtools (Quinlan and Hall
850 2010). First, a joint BED file containing the UTR and exon regions were made using awk and
851 sorted first by chromosome then by position. Using BEDtools these intervals were combined,
852 and intronic regions were calculated by finding regions in gene intervals not covered by either
853 UTR or exons. Intergenic spaces on each chromosome were calculated with the gene BED files
854 and chromosome sizes as inputs. GAT was then run for each chromosome in each assembly.

855

856 **Transposable Element Identification and Tracking**

857 The TransposonUltimate pipeline (Riehl et al. 2022) was run for both our N2 Bristol and CB4856
858 Hawaiian genome assemblies. MUST and SINE finder were run independently and integrated
859 into the filtering steps of the pipeline manually. Additionally, we added LTR retriever to the TE
860 identification ensemble to supplement LTR harvest and LTR finder. TE sequences that
861 overlapped with SNPs were identified using BEDtools. CB4856 Hawaiian SNPs were applied to
862 corresponding N2 Bristol TE sequences, and these sequences were cross-referenced with the
863 original TransposonUltimate output for CB4856 Hawaiian for matches. Unique polymorphic TE
864 sequences found in both genomes were then assessed for translocation events by examining
865 genomic start coordinates in each genome. Utilizing whole-genome alignments for each
866 chromosome, TEs were predicted to have moved if starting coordinates for each TE pair were
867 did not correspond to relative changes in coordinates due to alignment.

868

869

870

871 **Data Availability Statement**

872 The PacBio long-read and the Illumina short-read data generated in this study have been
873 submitted to the NCBI BioProject database (<https://www.ncbi.nlm.nih.gov/bioproject/>) under
874 accession number PRJNA907379. All custom scripts are available upon request. Strains are
875 available upon request.

876

877 **Acknowledgements**

878 We thank N. Kurhanewicz, C. Cahoon, E. Toraason, and J. Conery in the Libuda Lab for
879 thoughtful discussion and comments on the manuscript. We are grateful to the University of
880 Oregon's Genomics and Cell Characterization Core Facility for sample prep and sequencing of
881 our N2 Bristol and CB4856 Hawaiian strains. Over the course of many years beyond the time of

882 this study, thanks for inspiration from Walter Rogers and invaluable guidance from Dr. Glenn C.
883 Rowe given to Z.D.B.

884

885 **Funding**

886 This work was supported by the National Institutes of Health T32HD007348 to Z.D.B and
887 National Institutes of Health R35GM128890 and University of Oregon start-up funds to D.E.L.

888

889 **Conflict of Interest**

890 The authors declare no conflicts of interest.

891

892 **Author Contributions**

893 Z.D.B. polished primary genome assemblies, assessed genome quality, annotated the
894 genomes, and analyzed genomic variation and structures. A.F.S.N. helped conceive this study
895 and developed protocols for DNA purification, short-read Illumina sequencing, and variant
896 calling. D.D. developed protocols for long-read sequencing, devised strategies for genome
897 assembly, assembled the contigs and primary assembly, and filled gaps. C.A. identified
898 transposable elements and tracked copies containing SNPs between genome assemblies.
899 K.J.H. helped conceive this study, develop protocols for DNA purification, and purified the DNA
900 for the long-read PacBio sequencing. D.E.L. helped conceive this study, led discussions for the
901 comparison of different genomes, and coordinated work. All authors contributed to the
902 manuscript, with most of the writing by Z.D.B., A.S.F.N., and D.E.L.

903

904

905 **References**

906

907 Andersen, Erik C, Justin P Gerke, Joshua A Shapiro, Jonathan R Crissman, Rajarshi Ghosh,
908 Joshua S Bloom, Marie-Anne Félix, and Leonid Kruglyak. 2012. "Chromosome-Scale
909 Selective Sweeps Shape *Caenorhabditis Elegans* Genomic Diversity." *Nature Genetics*
910 44 (3): 285–90. <https://doi.org/10.1038/ng.1050>.

911 Bao, Weidong, Matthew G. Jurka, Vladimir V. Kapitonov, and Jerzy Jurka. 2009. "New
912 Superfamilies of Eukaryotic DNA Transposons and Their Internal Divisions." *Molecular
913 Biology and Evolution* 26 (5): 983–93. <https://doi.org/10.1093/molbev/msp013>.

914 Bessereau, Jean-Louis. 2006. "Transposons in *C. Elegans*." *WormBook : The Online Review of
915 C. Elegans Biology*, January, 1–13. <https://doi.org/10.1895/wormbook.1.70.1>.

916 Bolger, Anthony M, Marc Lohse, and Bjoern Usadel. 2014. "Trimmomatic: A Flexible Trimmer
917 for Illumina Sequence Data." *Bioinformatics (Oxford, England)* 30 (15): 2114–20.
918 <https://doi.org/10.1093/bioinformatics/btu170>.

919 C. elegans Sequencing Consortium. 1998. "Genome Sequence of the Nematode *C. Elegans*: A
920 Platform for Investigating Biology." *Science* 282 (5396): 2012–18.
921 <https://doi.org/10.1126/science.282.5396.2012>.

922 Carvalho, Claudia M B, and James R Lupski. 2016. "Mechanisms Underlying Structural Variant
923 Formation in Genomic Disorders." *Nature Reviews Genetics*. Nature Publishing Group.
924 <https://doi.org/10.1038/nrg.2015.25>.

925 Chalopin, Domitille, Magali Naville, Floriane Plard, Delphine Galiana, and Jean-Nicolas Volff.
926 2015. "Comparative Analysis of Transposable Elements Highlights Mobilome Diversity
927 and Evolution in Vertebrates." *Genome Biology and Evolution* 7 (2): 567–80.
928 <https://doi.org/10.1093/gbe/evv005>.

929 Crombie, Tim A, Stefan Zdraljevic, Daniel E Cook, Robyn E Tanny, Shannon C Brady, Ye
930 Wang, Kathryn S Evans, et al. 2019. "Deep Sampling of Hawaiian *Caenorhabditis
931 Elegans* Reveals High Genetic Diversity and Admixture with Global Populations." Edited
932 by Graham Coop, Diethard Tautz, and Asher Cutter. *eLife* 8 (December): e50465.
933 <https://doi.org/10.7554/eLife.50465>.

934 Danecek, Petr, Adam Auton, Goncalo Abecasis, Cornelis A Albers, Eric Banks, Mark A
935 DePristo, Robert E Handsaker, et al. 2011. "The Variant Call Format and VCFtools."
936 *Bioinformatics (Oxford, England)* 27 (15): 2156–58.
937 <https://doi.org/10.1093/bioinformatics/btr330>.

938 Danecek, Petr, and Shane A McCarthy. 2017. "BCFtools/Csq: Haplotype-Aware Variant
939 Consequences." *Bioinformatics (Oxford, England)* 33 (13): 2037–39.
940 <https://doi.org/10.1093/bioinformatics/btx100>.

941 Delcher, A L, S Kasif, R D Fleischmann, J Peterson, O White, and S L Salzberg. 1999.
942 "Alignment of Whole Genomes." *Nucleic Acids Research* 27 (11): 2369–76.
943 <https://doi.org/10.1093/nar/27.11.2369>.

944 Denver, Dee R, Peter C Dolan, Larry J Wilhelm, Way Sung, J Ignacio Lucas-Lledó, Dana K
945 Howe, Samantha C Lewis, et al. 2009. "A Genome-Wide View of *Caenorhabditis
946 Elegans* Base-Substitution Mutation Processes." *Proceedings of the National Academy
947 of Sciences of the United States of America* 106 (38): 16310–14.
948 <https://doi.org/10.1073/pnas.0904895106>.

949 Eide, D, and P Anderson. 1985. "Transposition of Tc1 in the Nematode *Caenorhabditis
950 Elegans*." *Proceedings of the National Academy of Sciences* 82 (6): 1756–60.
951 <https://doi.org/10.1073/pnas.82.6.1756>.

952 Emmons, Scott W., Lewis Yesner, Ke-san Ruan, and Daniel Katzenberg. 1983. "Evidence for a
953 Transposon in *Caenorhabditis Elegans*." *Cell* 32 (1): 55–65.
954 [https://doi.org/10.1016/0092-8674\(83\)90496-8](https://doi.org/10.1016/0092-8674(83)90496-8).

955 Feschotte, Cédric, and Ellen J. Pritham. 2007. "DNA Transposons and the Evolution of
956 Eukaryotic Genomes." *Annual Review of Genetics* 41: 331–68.
957 <https://doi.org/10.1146/annurev.genet.40.110405.090448>.

958 Fischer, Sylvia E J, Erno Wienholds, and Ronald H A Plasterk. 2003. "Continuous Exchange of
959 Sequence Information Between Dispersed Tc1 Transposons in the *Caenorhabditis*
960 *Elegans* Genome." *Genetics* 164 (1): 127–34.
961 <https://doi.org/10.1093/genetics/164.1.127>.

962 Garrison, Erik, and Gabor Marth. 2012. "Haplotype-Based Variant Detection from Short-Read
963 Sequencing." *arXiv*. <https://doi.org/10.48550/ARXIV.1207.3907>.

964 Gems, D, and D L Riddle. 2000. "Defining Wild-Type Life Span in *Caenorhabditis Elegans*." *The
965 Journals of Gerontology. Series A, Biological Sciences and Medical Sciences* 55 (5):
966 B215-9. <https://doi.org/10.1093/gerona/55.5.b215>.

967 Gilbert, Clément, Jean Peccoud, and Richard Cordaux. 2021. "Transposable Elements and the
968 Evolution of Insects." *Annual Review of Entomology* 66 (1): 355–72.
969 <https://doi.org/10.1146/annurev-ento-070720-074650>.

970 Girard, Lisa, and Michael Freeling. 1999. "Regulatory Changes as a Consequence of
971 Transposon Insertion." *Developmental Genetics* 25 (4): 291–96.
972 [https://doi.org/10.1002/\(SICI\)1520-6408\(1999\)25:4<291::AID-DVG2>3.0.CO;2-5](https://doi.org/10.1002/(SICI)1520-6408(1999)25:4<291::AID-DVG2>3.0.CO;2-5).

973 Goel, Manish, Hequan Sun, Wen-Biao Jiao, and Korbinian Schneeberger. 2019. "SyRI: Finding
974 Genomic Rearrangements and Local Sequence Differences from Whole-Genome
975 Assemblies." *Genome Biology* 20 (1): 277. <https://doi.org/10.1186/s13059-019-1911-0>.

976 Haraksingh, Rajini R, and Michael P Snyder. 2013. "Impacts of Variation in the Human Genome
977 on Gene Regulation." *Journal of Molecular Biology* 425 (21): 3970–77.
978 <https://doi.org/10.1016/j.jmb.2013.07.015>.

979 Heger, Andreas, Caleb Webber, Martin Goodson, Chris P Ponting, and Gerton Lunter. 2013.
980 "GAT: A Simulation Framework for Testing the Association of Genomic Intervals."
981 *Bioinformatics* 29 (16): 2046–48. <https://doi.org/10.1093/bioinformatics/btt343>.

982 Hodgkin, J, and T Doniach. 1997. "Natural Variation and Copulatory Plug Formation in
983 *Caenorhabditis Elegans*." *Genetics* 146 (1): 149–64.
984 <https://doi.org/10.1093/genetics/146.1.149>.

985 Hurles, Matthew E, Emmanouil T Dermitzakis, and Chris Tyler-Smith. 2008. "The Functional
986 Impact of Structural Variation in Humans." *Trends in Genetics : TIG* 24 (5): 238–45.
987 <https://doi.org/10.1016/j.tig.2008.03.001>.

988 James, Kent W, Baertsch Robert, Hinrichs Angie, Miller Webb, and Haussler David. 2003.
989 "Evolution's Cauldron: Duplication, Deletion, and Rearrangement in the Mouse and
990 Human Genomes." *Proceedings of the National Academy of Sciences* 100 (20): 11484–
991 89. <https://doi.org/10.1073/pnas.1932072100>.

992 Kamath, Ravi S, Andrew G Fraser, Yan Dong, Gino Poulin, Richard Durbin, Monica Gotta,
993 Alexander Kanapin, et al. 2003. "Systematic Functional Analysis of the *Caenorhabditis*
994 *Elegans* Genome Using RNAi." *Nature* 421 (6920): 231–37.
995 <https://doi.org/10.1038/nature01278>.

996 Kern, Andrew D, and Matthew W Hahn. 2018. "The Neutral Theory in Light of Natural
997 Selection." *Molecular Biology and Evolution* 35 (6): 1366–71.
998 <https://doi.org/10.1093/molbev/msy092>.

999 Kim, Bernard Y, Jeremy R Wang, Danny E Miller, Olga Barmina, Emily Delaney, Ammon
1000 Thompson, Aaron A Comeault, et al. 2021. "Highly Contiguous Assemblies of 101
1001 Drosophilid Genomes." Edited by Graham Coop, Patricia J Wittkopp, and Timothy B
1002 Sackton. *eLife* 10: e66405. <https://doi.org/10.7554/eLife.66405>.

1003 Kim, Chuna, Jun Kim, Sunghyun Kim, Daniel E Cook, Kathryn S Evans, Erik C Andersen, and
1004 Junho Lee. 2019. "Long-Read Sequencing Reveals Intra-Species Tolerance of
1005 Substantial Structural Variations and New Subtelomere Formation in *C. Elegans*." *Genome*
1006 *Research* 29 (6): 1023–35. <https://doi.org/10.1101/gr.246082.118>.

1007 Koch, R, H G van Luenen, M van der Horst, K L Thijssen, and R H Plasterk. 2000. "Single
1008 Nucleotide Polymorphisms in Wild Isolates of *Caenorhabditis Elegans*." *Genome*
1009 *Research* 10 (11): 1690–96. <https://doi.org/10.1101/gr.gr-1471r>.

1010 Koren, Sergey, Brian P Walenz, Konstantin Berlin, Jason R Miller, Nicholas H Bergman, and
1011 Adam M Phillippy. 2017. "Canu: Scalable and Accurate Long-Read Assembly via
1012 Adaptive k-Mer Weighting and Repeat Separation." *Genome Research* 27 (5): 722–36.
1013 <https://doi.org/10.1101/gr.215087.116>.

1014 Lappalainen, Tuuli, Alexandra J. Scott, Margot Brandt, and Ira M. Hall. 2019. "Genomic Analysis
1015 in the Age of Human Genome Sequencing." *Cell* 177 (1): 70–84.
1016 <https://doi.org/10.1016/j.cell.2019.02.032>.

1017 Laricchia, K.M., S. Zdraljevic, D.E. Cook, and E.C. Andersen. 2017. "Natural Variation in the
1018 Distribution and Abundance of Transposable Elements Across the *Caenorhabditis*
1019 *Elegans* Species." *Molecular Biology and Evolution* 34 (9): 2187–2202.
1020 <https://doi.org/10.1093/molbev/msx155>.

1021 Lee, Daehan, Stefan Zdraljevic, Lewis Stevens, Ye Wang, Robyn E. Tanny, Timothy A.
1022 Crombie, Daniel E. Cook, et al. 2021. "Balancing Selection Maintains Hyper-Divergent
1023 Haplotypes in *Caenorhabditis Elegans*." *Nature Ecology & Evolution* 5 (6): 794–807.
1024 <https://doi.org/10.1038/s41559-021-01435-x>.

1025 Lee, Heng-Chi, Weifeng Gu, Masaki Shirayama, Elaine Youngman, Darryl Conte, and Craig C.
1026 Mello. 2012. "*C. Elegans* piRNAs Mediate the Genome-Wide Surveillance of Germline
1027 Transcripts." *Cell* 150 (1): 78–87. <https://doi.org/10.1016/j.cell.2012.06.016>.

1028 Lesack, Kyle, Grace M. Mariene, Erik C. Andersen, and James D. Wasmuth. 2022. "Different
1029 Structural Variant Prediction Tools Yield Considerably Different Results in
1030 *Caenorhabditis Elegans*." *PLOS ONE* 17 (12): e0278424.
1031 <https://doi.org/10.1371/journal.pone.0278424>.

1032 Li, Heng. 2018. "Minimap2: Pairwise Alignment for Nucleotide Sequences." *Bioinformatics* 34
1033 (18): 3094–3100. <https://doi.org/10.1093/bioinformatics/bty191>.

1034 Li, Heng, and Richard Durbin. 2009. "Fast and Accurate Short Read Alignment with Burrows–
1035 Wheeler Transform." *Bioinformatics* 25 (14): 1754–60.
1036 <https://doi.org/10.1093/bioinformatics/btp324>.

1037 Li, Heng, Bob Handsaker, Alec Wysoker, Tim Fennell, Jue Ruan, Nils Homer, Gabor Marth,
1038 Goncalo Abecasis, Richard Durbin, and 1000 Genome Project Data Processing
1039 Subgroup. 2009. "The Sequence Alignment/Map Format and SAMtools." *Bioinformatics*
1040 (Oxford, England) 25 (16): 2078–79. <https://doi.org/10.1093/bioinformatics/btp352>.

1041 Liao, L. W., B. Rosenzweig, and D. Hirsh. 1983. "Analysis of a Transposable Element in
1042 *Caenorhabditis Elegans*." *Proceedings of the National Academy of Sciences of the*
1043 *United States of America* 80 (12): 3585–89. <https://doi.org/10.1073/pnas.80.12.3585>.

1044 Mahmoud, Medhat, Nastassia Gobet, Diana Ivette Cruz-Dávalos, Ninon Mounier, Christophe
1045 Dessimoz, and Fritz J Sedlazeck. 2019. "Structural Variant Calling: The Long and the
1046 Short of It." *Genome Biology* 20 (1): 246. <https://doi.org/10.1186/s13059-019-1828-7>.

1047 Manni, Mose, Matthew R Berkeley, Mathieu Seppey, Felipe A Simão, and Evgeny M Zdobnov.
1048 2021. "BUSCO Update: Novel and Streamlined Workflows along with Broader and
1049 Deeper Phylogenetic Coverage for Scoring of Eukaryotic, Prokaryotic, and Viral
1050 Genomes." *Molecular Biology and Evolution* 38 (10): 4647–54.
1051 <https://doi.org/10.1093/molbev/msab199>.

1052 Maydan, Jason S, Adam Lorch, Mark L Edgley, Stephane Flibotte, and Donald G Moerman.
1053 2010. "Copy Number Variation in the Genomes of Twelve Natural Isolates of

1054 1055 1056 1057 1058 1059 1060 1061 1062 1063 1064 1065 1066 1067 1068 1069 1070 1071 1072 1073 1074 1075 1076 1077 1078 1079 1080 1081 1082 1083 1084 1085 1086 1087 1088 1089 1090 1091 1092 1093 1094 1095 1096 1097 1098 1099 1100 1101 1102

Caenorhabditis Elegans." *BMC Genomics* 11 (January): 62.
<https://doi.org/10.1186/1471-2164-11-62>.

McKenna, Aaron, Matthew Hanna, Eric Banks, Andrey Sivachenko, Kristian Cibulskis, Andrew Kernytsky, Kiran Garimella, et al. 2010. "The Genome Analysis Toolkit: A MapReduce Framework for Analyzing next-Generation DNA Sequencing Data." *Genome Research* 20 (9): 1297–1303. <https://doi.org/10.1101/gr.107524.110>.

Miller, Danny E, Kevin R Cook, and R Scott Hawley. 2019. "The Joy of Balancers." *PLOS Genetics* 15 (11): e1008421.

Muzzey, Dale, Eric A Evans, and Caroline Lieber. 2015. "Understanding the Basics of NGS: From Mechanism to Variant Calling." *Current Genetic Medicine Reports* 3 (4): 158–65. <https://doi.org/10.1007/s40142-015-0076-8>.

Nattestad, Maria, and Michael C Schatz. 2016. "Assemblytics: A Web Analytics Tool for the Detection of Variants from an Assembly." *Bioinformatics (Oxford, England)* 32 (19): 3021–23. <https://doi.org/10.1093/bioinformatics/btw369>.

Nicholas, W L, E C Dougherty, and E L Hansen. 1959. "Axenic Cultivation of Caenorhabditis Briggsae (Nematoda: Rhabditidae) with Chemically Undefined Supplements; Comparative Studies with Related Nematodes." *Ann. N. Y. Acad. Sci* 77: 218–36.

Plasterk, Ronald H.A, Zsuzsanna Izsvák, and Zoltán Ivics. 1999. "Resident Aliens: The Tc1/Mariner Superfamily of Transposable Elements." *Trends in Genetics* 15 (8): 326–32. [https://doi.org/10.1016/S0168-9525\(99\)01777-1](https://doi.org/10.1016/S0168-9525(99)01777-1).

Quinlan, Aaron R, and Ira M Hall. 2010. "BEDTools: A Flexible Suite of Utilities for Comparing Genomic Features." *Bioinformatics* 26 (6): 841–42. <https://doi.org/10.1093/bioinformatics/btq033>.

Riehl, Kevin, Cristian Riccio, Eric A Miska, and Martin Hemberg. 2022. "TransposonUltimate: Software for Transposon Classification, Annotation and Detection." *Nucleic Acids Research* 50 (11): e64–e64. <https://doi.org/10.1093/nar/gkac136>.

Rockman, Matthew V, and Leonid Kruglyak. 2009. "Recombinational Landscape and Population Genomics of Caenorhabditis Elegans." *PLOS Genetics* 5 (3): e1000419.

Sakamoto, Yoshitaka, Suzuko Zaha, Yutaka Suzuki, Masahide Seki, and Ayako Suzuki. 2021. "Application of Long-Read Sequencing to the Detection of Structural Variants in Human Cancer Genomes." *Computational and Structural Biotechnology Journal* 19: 4207–16. <https://doi.org/10.1016/j.csbj.2021.07.030>.

Sarsani, Vishal Kumar, Narayanan Raghupathy, Ian T Fiddes, Joel Armstrong, Francoise Thibaud-Nissen, Oraya Zinder, Mohan Bolisetty, et al. 2019. "The Genome of C57BL/6J 'Eve', the Mother of the Laboratory Mouse Genome Reference Strain." *G3 (Bethesda, Md.)* 9 (6): 1795–1805. <https://doi.org/10.1534/g3.119.400071>.

Shumate, Alaina, and Steven L Salzberg. 2021. "Liftoff: Accurate Mapping of Gene Annotations." *Bioinformatics* 37 (12): 1639–43. <https://doi.org/10.1093/bioinformatics/btaa1016>.

Sijen, Titia, and Ronald H. A. Plasterk. 2003. "Transposon Silencing in the Caenorhabditis Elegans Germ Line by Natural RNAi." *Nature* 426 (6964): 310–14. <https://doi.org/10.1038/nature02107>.

Simão, Felipe A, Robert M Waterhouse, Panagiotis Ioannidis, Evgenia V Kriventseva, and Evgeny M Zdobnov. 2015. "BUSCO: Assessing Genome Assembly and Annotation Completeness with Single-Copy Orthologs." *Bioinformatics* 31 (19): 3210–12. <https://doi.org/10.1093/bioinformatics/btv351>.

Slotkin, R. Keith, and Robert Martienssen. 2007. "Transposable Elements and the Epigenetic Regulation of the Genome." *Nature Reviews Genetics* 8 (4): 272–85. <https://doi.org/10.1038/nrg2072>.

1103 Stankiewicz, Paweł, and James R Lupski. 2010. "Structural Variation in the Human Genome
1104 and Its Role in Disease." *Annual Review of Medicine* 61 (1): 437–55.
1105 <https://doi.org/10.1146/annurev-med-100708-204735>.

1106 Stewart, Mary K, Nathaniel L Clark, Gennifer Merrihew, Evan M Galloway, and James H
1107 Thomas. 2005. "High Genetic Diversity in the Chemoreceptor Superfamily of
1108 *Caenorhabditis Elegans*." *Genetics* 169 (4): 1985–96.
1109 <https://doi.org/10.1534/genetics.104.035329>.

1110 Stranger, Barbara E., Forrest Matthew S., Dunning Mark, Ingle Catherine E., Beazley Claude,
1111 Thorne Natalie, Redon Richard, et al. 2007. "Relative Impact of Nucleotide and Copy
1112 Number Variation on Gene Expression Phenotypes." *Science* 315 (5813): 848–53.
1113 <https://doi.org/10.1126/science.1136678>.

1114 Sudmant, Peter H, Tobias Rausch, Eugene J Gardner, Robert E Handsaker, Alexej Abyzov,
1115 John Huddleston, Yan Zhang, et al. 2015. "An Integrated Map of Structural Variation in
1116 2,504 Human Genomes." *Nature* 526 (7571): 75–81.
1117 <https://doi.org/10.1038/nature15394>.

1118 Sulston, J E, and S Brenner. 1974. "The DNA of *Caenorhabditis Elegans*." *Genetics* 77 (1): 95–
1119 104. <https://doi.org/10.1093/genetics/77.1.95>.

1120 Surzycki, S A, and W R Belknap. 2000. "Repetitive-DNA Elements Are Similarly Distributed on
1121 *Caenorhabditis Elegans* Autosomes." *Proceedings of the National Academy of Sciences
1122 of the United States of America* 97 (1): 245–49. <https://doi.org/10.1073/pnas.97.1.245>.

1123 Swan, Kathryn A, Damian E Curtis, Kathleen B McKusick, Alexander V Voinov, Felipa A Mapa,
1124 and Michael R Cancilla. 2002. "High-Throughput Gene Mapping in *Caenorhabditis
1125 Elegans*." *Genome Research* 12 (7): 1100–1105. <https://doi.org/10.1101/gr.208902>.

1126 Thomas, Cristel G, Wei Wang, Richard Jovelin, Rajarshi Ghosh, Tatiana Lomasko, Quang
1127 Trinh, Leonid Kruglyak, Lincoln D Stein, and Asher D Cutter. 2015. "Full-Genome
1128 Evolutionary Histories of Selfing, Splitting, and Selection in *Caenorhabditis*." *Genome
1129 Research* 25 (5): 667–78. <https://doi.org/10.1101/gr.187237.114>.

1130 Thompson, Owen A, L Basten Snoek, Harm Nijveen, Mark G Sterken, Rita J M Volkers, Rachel
1131 Brenchley, Arjen van't Hof, et al. 2015. "Remarkably Divergent Regions Punctuate the
1132 Genome Assembly of the *Caenorhabditis Elegans* Hawaiian Strain CB4856." *Genetics*
1133 200 (3): 975–89. <https://doi.org/10.1534/genetics.115.175950>.

1134 Van't Hof, Arjen E, Pascal Campagne, Daniel J Rigden, Carl J Yung, Jessica Lingley, Michael A
1135 Quail, Neil Hall, Alistair C Darby, and Ilik J Saccheri. 2016. "The Industrial Melanism
1136 Mutation in British Peppered Moths Is a Transposable Element." *Nature* 534 (7605):
1137 102–5. <https://doi.org/10.1038/nature17951>.

1138 Vergara, Ismael A, Allan K Mah, Jim C Huang, Maja Tarailo-Graovac, Robert C Johnsen, David
1139 L Baillie, and Nansheng Chen. 2009. "Polymorphic Segmental Duplication in the
1140 Nematode *Caenorhabditis Elegans*." *BMC Genomics* 10 (1): 329.
1141 <https://doi.org/10.1186/1471-2164-10-329>.

1142 Wicks, Stephen R, Raymond T Yeh, Warren R Gish, Robert H Waterston, and Ronald H A
1143 Plasterk. 2001. "Rapid Gene Mapping in *Caenorhabditis Elegans* Using a High Density
1144 Polymorphism Map." *Nature Genetics* 28 (2): 160–64. <https://doi.org/10.1038/88878>.

1145 Yoshimura, Jun, Kazuki Ichikawa, Massa J Shoura, Karen L Artiles, Idan Gabdank, Lamia
1146 Wahba, Cheryl L Smith, et al. 2019. "Recompleting the *Caenorhabditis Elegans*
1147 Genome." *Genome Research* 29 (6): 1009–22. <https://doi.org/10.1101/gr.244830.118>.

1148 Zhao, Yuehui, Lijiang Long, Wen Xu, Richard F Campbell, Edward E Large, Joshua S Greene,
1149 and Patrick T McGrath. 2018. "Changes to Social Feeding Behaviors Are Not Sufficient
1150 for Fitness Gains of the *Caenorhabditis Elegans* N2 Reference Strain." *eLife* 7 (October).
1151 <https://doi.org/10.7554/eLife.38675>.

1152